



# Protein scaffolds: A tool for multi-enzyme assembly

Shubhada Gad, Sonal Ayakar\*

Department of Biotechnology, Institute of Chemical Technology - IndianOil Odisha Campus Bhubaneswar, Odisha 751013, India

## ARTICLE INFO

### Keywords:

Protein scaffolds  
Multi-enzyme complex  
Binding modules  
Dockerin-cohesin interactions  
SpyTag-SpyCatcher system

## ABSTRACT

The synthesis of complex molecules using multiple enzymes simultaneously in one reaction vessel has rapidly emerged as a new frontier in the field of bioprocess technology. However, operating different enzymes together in a single vessel limits their operational performance which needs to be addressed. With this respect, scaffolding proteins play an immense role in bringing different enzymes together in a specific manner. The scaffolding improves the catalytic performance, enzyme stability and provides an optimal micro-environment for biochemical reactions. This review describes the components of protein scaffolds, different ways of constructing a protein scaffold-based multi-enzyme complex, and their effects on enzyme kinetics. Moreover, different conjugation strategies viz; dockerin-cohesin interaction, SpyTag-SpyCatcher system, peptide linker-based ligation, affibody, and sortase-mediated ligation are discussed in detail. Various analytical and characterization tools that have enabled the development of these scaffolding strategies are also reviewed. Such mega-enzyme complexes promise wider applications in the field of biotechnology and bioengineering.

## 1. Introduction

Nature has always witnessed the highly organized enzymatic complexes that drive various metabolic reactions with a high degree of specificity. Indeed, in its highly ordered form, enzymes work more efficiently with better substrate channeling which subsequently enhances the overall productivity [1]. Such multi-enzyme clusters are often formed with the aid of scaffolds wherein enzymes assemble on desired docking sites on the scaffold biomolecule. Thus, the scaffolded clusters play an immense role in carrying out multi-step biochemical reactions. In recent decades, biocatalysis has been gaining considerable attention owing to its sustainable and environmentally friendly nature that in turn provides a greener alternative to traditional chemical synthesis. Tremendous efforts have been made in the field of biocatalyst engineering and biomimetics to design such multi-enzyme nanostructures resembling the naturally occurring scaffolded multi-enzyme complexes which would catalyze industrially relevant biochemical reactions with an enhanced rate of productivity. Several types of scaffold materials and technologies have been investigated to improve the overall processivity, stability, and substrate accessibility of enzymes along with the aim of increasing the enzyme loading capacity of scaffold materials. These improvements compensate for the high cost of enzyme biocatalyst in biotechnological industries.

Scaffolding material can be classified into two categories: synthetic

scaffolds and natural macromolecular scaffolds (Table 1). In the context of synthetic scaffolds, diverse nanomaterials with a high aspect ratio (ratio of surface area to volume) have been explored to improve enzyme loading and thereby reducing the diffusional barrier. This strategy provides better conversion yield and improved catalytic activity [2]. To date, numerous versatile nanomaterials such as nanotubes [3], nanowires [4], nanoparticles [5], nanosponges [6], nanoflowers [7], metal-organic frameworks [8], nanocages [9], and nanocomposites [10] have been reported to be utilized for the construction of artificial scaffolds for enzyme cascades.

Natural macromolecular scaffolds have also been widely employed where nucleic acids and proteins are used as scaffold materials. For instance, DNA, as well as RNA in their one or two-dimensional geometries, organizes the enzyme cascades into a complex by using well-established nucleic acid-based methodologies [20, 22]. However nucleic acid-based nanoscaffolds often suffer from the high cost of synthesis along with the struggle of docking the enzymes on it without affecting their biocatalytic activity [23]. On the other hand, proteins can be an interesting alternative candidate for the localization of enzyme/s since they can be genetically modified, can be produced in large quantities in heterologous hosts, and can be conjugated with the enzyme/s by integration of simple molecular recognition domain [24]. Thus, a diverse range of proteins has been explored to develop a versatile scaffold system for achieving the desirable productivity of the metabolic

\* Corresponding author.

E-mail address: [sr.ayakar@iocb.ictmumbai.edu.in](mailto:sr.ayakar@iocb.ictmumbai.edu.in) (S. Ayakar).

<https://doi.org/10.1016/j.btre.2021.e00670>

Received 15 July 2021; Received in revised form 13 August 2021; Accepted 3 September 2021

Available online 6 September 2021

2215-017X/© 2021 The Authors. Published by Elsevier B.V. This is an open access article under the CC BY license (<http://creativecommons.org/licenses/by/4.0/>).

**Table 1**  
Scaffold materials utilized for enzyme immobilization and their potential applications.

Scaffold type	Scaffold material	Enzymes immobilized	Application	Reference
Synthetic scaffolds	Polystyrene nanospheres	Endoglucanase	Biofuel production	[11]
	CeO <sub>2</sub> -TiO <sub>2</sub> Nanocomposites	Lactate oxidase	Electrochemical biosensors	[10]
	Zirconium based Metal-Organic Frameworks	Cellulase	Biomass valorization	[12]
	Multi-walled carbon nanotube	Lipase	Synthesis of fruit flavors	[3]
	Chitosan magnetic nanoparticles	Pectinase	Clarification and stabilization of fruit juices	[13]
	SBA-15 mesoporous sieves	Acetylcho linesterase	Detection of organophosphorus and carbamate pesticide	[14]
Biological supramolecular scaffolds	Polyhydroxyalkanoates(PHA)	Organophosphorus anhydride hydrolase	Bioremediation	[15]
	Magnetosomes	$\beta$ - glucuronidase	Biomedical application	[16]
	Bacteriophages P22 virus-like particles (VLPs)	Peroxygenase CYP <sub>BM3</sub> 21B3 and Glucose oxidase	Biotransformation of endocrine disruptor compounds	[17]
	Forisomes	Glucose-6-phosphate dehydrogenase and Hexokinase 2	Biosensor and microfluidic devices	[18]
	Apoferritin	Human carbonic anhydrase, Retro-aldolase, and Kemp eliminase	Pharmaceutical and nanotechnological application	[19]
	RNA scaffold	(FeFe)-hydrogenase and ferredoxin	Hydrogen production	[20]
	DNA nanostructure	Glucose oxidase and horseradish peroxidase	Biosensor and biotechnological application	[21]

pathway. In this review, we highlight various ways of enzyme assembly on a protein backbone, different molecular recognition strategies for protein-enzyme conjugation, and characterization of the whole complex. We then discuss diverse novel protein assemblies that have been exploited so far as a scaffolding platform for multi-enzyme assembly.

## 2. Protein scaffold system

In nature, scaffold proteins are involved in signaling cascades where they serve docking sites for various protein members of the signaling cascade thereby smoothing out corresponding interactions and functions [25]. Being genetically modifiable; such nanoscale protein-based carriers could efficiently organize complex enzyme cascades comprising two or more types of enzymes in specified configuration, subsequently improving the enzymatic performance along with the pathway flux [26]. Furthermore, the scaffold-based multi-enzyme complex also decreases the loss of intermediates due to proximity of catalytic sites, decreases overall transit time, and reduces product feedback inhibition [27, 28].

Cellulosome is one such distinctive example of a naturally occurring protein scaffold system comprising structural backbone (scaffoldins) where cellulases have been localized via dockerin-cohesin interactions [29]. Owing to better catalytic efficiency and highly organized structure, cellulosomes have potential applications in various biorefineries [30]. To date, various researchers have used the scaffoldin and interactive domains from natural cellulosomes for the colocalization of various enzymes. For instance, alcohol dehydrogenase (ADH), formate dehydrogenase, and formaldehyde dehydrogenase have been assembled on scaffoldin for NADH production whereas amidohydrolase and hydantoinase assembled for semi-synthetic antibiotic production [31,

32].

Different strategies that are applied to design protein scaffold systems are depicted in Fig. 1. The basic structural units of protein scaffolds are adapter domain, peptide motifs/ligands, and linker. These three building blocks of the scaffold system affect the overall shape of the scaffold [33]. Adapter domains are small protein-binding modules of adapter proteins that permit specific protein-protein interactions in a highly regulated fashion. Phosphotyrosine binding domain, Src homology 2, and Src homology 3 domains are few well-known examples of adapter domains [34]. Peptide motifs or ligands are linear interactive peptides having short amino acid sequences complementary to adapter domains. Linkers act as connecting bridges between engineered enzymes and attached peptide motifs (Fig. 1a). Alternatively, peptide ligands can also be directly fused with enzymes eliminating the use of linkers for the development of scaffold systems (Fig. 1b). On the contrary, enzymes can be directly fused with scaffold proteins via linkers for the building of multi-enzyme complexes (Fig. 1c). Lastly, linkers can be directly used to interlink the multiple enzymes with each other to form multi-enzyme complexes (Fig. 1d). While selecting a particular method for enzyme scaffolding, one must consider the kind of enzyme/s (type/s as well as copy number) to be immobilized and their substrate-enzyme reaction/s as it may block active sites of enzyme/s and affect overall reaction kinetics respectively if the selected method is unsuitable for enzyme cascade.

## 3. Strategies of enzyme immobilization on a protein scaffold

There are two general ways of enzyme immobilization using protein nanocarrier viz; surface localization and encapsulation. In both cases, enzymes can be covalently or non-covalently associated with their

scaffold protein. Following are some recent strategies applied for the ligation of enzymes to scaffold protein (Fig. 2).

### 3.1. Dockerin-cohesin interaction

Dockerin-cohesin interactions are a vital part of the cellulosome where cohesin modules are associated with scaffoldin and are responsible for organizing the cellulolytic enzymes. Whereas, dockerin bearing enzymes anchor to the scaffoldin via high-affinity dockerin-cohesin interactions having dissociation constant ( $K_d$ ) ranging from  $10^{-9}$  M to  $10^{-12}$  M [35, 36].  $Ca^{+2}$  ions are essential for the interactions due to the presence of calcium-binding motif in the dockerin domain [37]. Karpol et al. have developed an affinity-based protein purification system using dockerin-cohesin interactions where cohesin module was immobilized on the beaded cellulose (affinity resin matrix) via carbohydrate-binding domain and targeted protein was tagged with truncated dockerin (affinity tag). The targeted protein binds to the column matrix through dockerin-cohesin interactions that later effectively eluted out using gradients of EDTA. Reutilization study further confirms the reusable nature of the affinity matrix for protein purification [38].

Dockerin-cohesin interactions were used to construct a cytosolic synthetic scaffold system in *Saccharomyces cerevisiae* for the production of 2,3-butanediol in another study. This increased the production titer by 37% [39]. Similarly, improvement of xylitol production was achieved by displaying xylose reductase (XR) and phosphite dehydrogenase (PTDH) on the outer coat protein (CotG) of *Bacillus subtilis* spores by controlling the XR/PTDH stoichiometry. XR and PTDH copy number on the spore surface was controlled by using a dockerin-cohesin module from two different sources viz; *Clostridium thermocellum* type 1 dockerin-cohesin module for XR and *Ruminococcus flavefecians* type 1 dockerin-cohesin module for PTDH. Furthermore, the stability of XR and PTDH was improved by 2.8-fold and 2.3-fold respectively at 25 °C after 10 h of incubation [40].

### 3.2. SpyTag-SpyCatcher system

The Howarth laboratory has developed the SpyTag-SpyCatcher domain system that is widely used for the colocalization of different enzymes [41, 42]. This system is formed by splitting the CnaB2 domain of the surface protein (FbaB) of *Streptococcus pyogenes*. SpyTag is a short, unfolded, versatile 13 amino acids long peptide sequence consisting of reactive aspartic acid residue which upon recognition of reactive lysine residue of its partner protein i.e. SpyCatcher, forms a covalent isopeptide bond [43]. The chemistry of the SpyTag-SpyCatcher bioconjugation process has been substantiated to be very rapid, highly efficient, independent of its position on the protein sequence, and highly robust in nature with stability at wide reaction conditions of temperature (4–37 °C), pH (4–8), and in the presence of various detergents (Tween-100, Tween-20, CHAPS, Nonidet P-40 except SDS) [44].

Jia et al. have constructed a polymeric SpyCatcher scaffold whose feasibility was initially inspected by conjugating SpyTagged enzymes (endoxyranase and arabinofuranosidase) on polymeric SpyCatcher construct in a site-specific and ratio-controllable manner and achieved 53% higher sugar conversion yield [45]. The construct was further explored for the detection of ovalbumin in ELISA by conjugation of SpyTagged Nanoluc and protein G on the scaffold [45]. Another research group has developed a single-step method for the purification and immobilization of xylanase-lichenase chimera [46]. SpyTag was fused between xylanase and lichenase to form a chimera that covalently binds to SpyCatcher-elastin like polypeptides (purification tag) via *in vitro* spontaneous SpyTag-SpyCatcher reaction and simultaneously self-assembled to form insoluble active particles during purification process which serves as immobilized enzyme complex. This immobilized enzyme chimera improved the stability by retaining 44% and 56% activities of xylanase and lichenase respectively even after 10 subsequent reaction cycles. However, a 1.7-fold (xylanase) and 1.1-fold (lichenase)

decrease in the catalytic efficiency of immobilized enzyme was found [46].

Dovala et al. demonstrated SpyCatcher-SpyTag based rapid analysis of proteins where fluorophore tagged SpyCatcher binds to SpyTagged target proteins from cell lysate by SpyCatcher-SpyTag interactions during the pre-incubation period before electrophoresis [47]. Direct fluorescence imaging of gel following electrophoretic protein separation gives highly specific western blot-like information with the least reagents. Furthermore, this fluorophore-SpyCatcher was effectively used to analyze mono-dispersity, expression level, aggregation state, and solubility of tagged protein using fluorescence size exclusion chromatography before any purification [47]. Overall, these examples prove the utility of the versatile, robust SpyCatcher-SpyTag system in biotechnological and analytical fields.

### 3.3. Peptide linker mediated ligation

Two or more enzymes are genetically fused through short peptide bridges to create scaffolded multi-enzyme cascades. Such short peptide linkers could effectively facilitate better substrate channeling between the fused enzymes [48]. Haga et al. demonstrated the effect of linker on the monooxygenase activity of proliferating cell nuclear antigen (PCNA)-based multi-enzyme complex comprising of *Pseudomonas putida* cytochrome P450 (P450cam), putidaredoxin reductase (PdR), and putidaredoxin (PdX). In this study, authors examined the effect of the poly-L-proline-rich linker between PCNA subunit 2 and PdX and reported 1.9 fold improvement in the overall monooxygenase activity [49]. Furthermore, the effect of flexible (Glycine)<sub>4</sub>-(Serine) repeating linker on the monooxygenase activity was explored with no change in the individual activities [49]. In another example, the effect of linker configuration on the structure and activity of formate dehydrogenase and leucine dehydrogenase in terms of linker type (rigid or flexible) and copy number was exploited and increased enzyme activity and thermal stability of fused enzymes were obtained with rigid peptide linker than flexible linker [50]. Both the findings suggest that rigid peptide linkers are more appropriate for improving catalytic performance and to fine-tune spatial arrangement of enzymes in multi-enzyme complex [49, 50]. Linkers have been widely used for improving the direct channeling of intermediates between catalytic modules of polyketide synthase [51, 52]. Also, this approach has been successfully implemented for the synthesis of bifunctional enzymes mainly for cost-effective recycling of co-factors [53, 54, 50].

### 3.4. Affibodies

Affibodies are relatively smaller (6 kDa) and less complex immunoglobulin-like affinity proteins consisting of 58 non-cysteine residues of three-helix bundle domains derived from the Z domain of protein A from *Staphylococcus aureus* [55]. The phage display technique is used for the production of randomized phage display affibody libraries to create ligand binding variants from which high-affinity ligand binding affibody is selected after bio-panning [56, 57]. These affibody molecules are known to have fast-folding kinetics with extreme pH and temperature stability that make them a favorable tool for scaffolding enzyme cascades. For scaffolding multiple enzymes, affibody: anti-idiotypic affibody binding pairs are used where anti-idiotypic affibodies are raised against affibodies to form high-affinity interaction with  $K_d$  value of 0.05  $\mu$ M to 0.9  $\mu$ M [58, 59]. Eklund et al. have designed staphylococcal protein A based scaffold that mimics the architecture of cellulosomes where engineered affibody:Ig-binding domain interactions replace dockerin-cohesin interactions. This designer cellulosome, when fused with carbohydrate-binding domain, binds efficiently to the cellulose surface. However, enzyme assembly on designer cellulosome and its effect on enzyme kinetics were not examined under this study [60].

Few reports are available stating colocalization of enzymes using affibody:anti-idiotypic affibody pairs on synthetic scaffold proteins. In

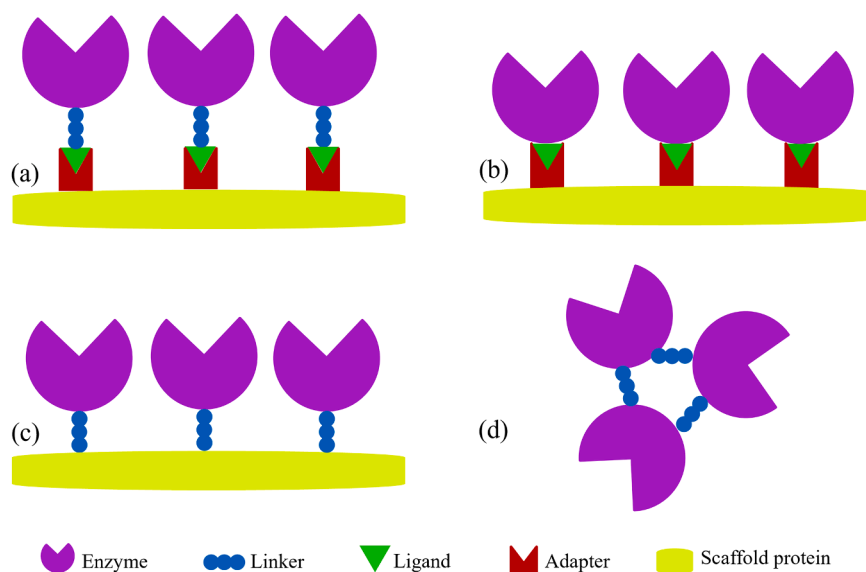


**Fig. 1.** Enzyme scaffolding strategies; (a) Adapter domain-ligand mediated enzyme assembly on scaffold protein with peptide linker as a connecting bridge; (b) Direct assembly of enzymes on scaffold protein through adapter domain-ligand interactions; (c) Direct fusion of enzymes on scaffold protein via peptide linker; (d) Peptide linker based enzyme cross-linking.

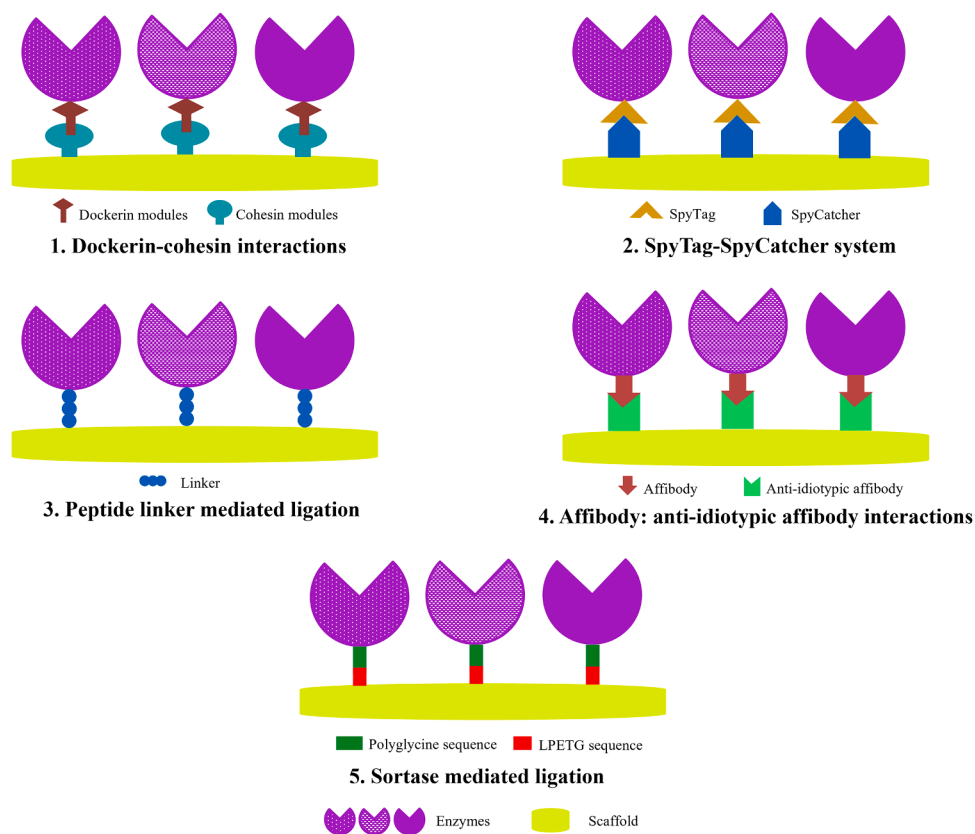


**Fig. 2.** Overview of recent enzyme-protein ligation strategies.

one such study, a bifunctional enzyme scaffold was formed by linking two different anti-idiotypic affibodies (anti-Z<sub>Taq</sub> and anti-Z<sub>IgA</sub>) on which affibody fused enzymes (Z<sub>Taq</sub> fused farnesene synthase and Z<sub>IgA</sub> fused farnesyl diphosphate synthase) were localized *in vivo* by affibody:anti-idiotypic affibody interactions in *S. cerevisiae* and 135% increase in yield of farnesene was achieved [59]. This strategy was further extended to three enzyme cascades of the poly-hydroxybutyrate pathway in

*Escherichia coli* and resulted in a seven-fold increase in poly-hydroxybutyrate yield [59]. This finding further potentiates the use of affibodies in the field of metabolic engineering.

### 3.5. Sortase mediated ligation

Enzyme-mediated protein-protein ligation is another popular

strategy of bioconjugation of enzymes to the protein scaffold structure. Sortase A is one such enzyme that assists isopeptide bond formation between the proteins of interest. Sortase A is membrane-bound cysteine transpeptidase expressed by *Staphylococcus aureus* [61]. In the presence of  $\text{Ca}^{+2}$ , sortase A first recognizes its substrate *i.e.* peptide motif LPXTG, normally fused with protein to be ligated at its C-terminal region. Immediately upon recognition, it cleaves the LPXTG peptide sequence between the peptide bond of threonine and glycine leading to the formation of thioester intermediate. Afterward, another nucleophilic substrate of sortase A *i.e.* N-terminal oligo glycine peptide tag of the second target protein reacts with thioester intermediate by nucleophilic attack leading to the ligation of the target proteins by isopeptide bond formation thereby liberating ligated proteins and free sortase A enzyme [62]. Though the entire process seems to be convenient for scaffolding enzyme cascade, the low binding affinity ( $K_m$  value  $>5.0$  mM), poor reaction kinetics extending reaction time, and lowering ligation efficiency constrain the widespread adoption of this strategy [63].

Utilizing a high molar concentration of enzyme as well as nucleophilic peptide substrate could enhance the ligation efficiency but at the expense of high cost. The consequences of such an approach may not be economically feasible for constructing scaffold systems for industrial applications. However, advancement in protein engineering has surpassed the limitations of sortase A [64, 65, 66]. Alternatively, a proximity-based sortase A mediated ligation approach with 95% ligation efficiency can be used for bioconjugation [67]. Sakamoto et al. attempted to ligate luciferase, alkaline phosphatase, and glucose oxidase (GOx) on the ZZ domain using sortase A with no significant effect on the enzyme activities [68]. Whereas, metabolic channeling of pyruvate formate lyase and phosphate acetyltransferase through sortase A mediated ligation diverts the central metabolic flux towards the acetate in the cytoplasm of *E. coli* [69]. Similarly, McConnell and co-workers have designed nanocage (T33-21) as a scaffold to exploit cellulase synergy utilizing colocalization of Cel48S exoglucanase and Cel8A endoglucanase from *C. thermocellum*, where enzymes were tagged with short polyglycine peptide whereas, LPXTG sequence was fused with scaffold backbone for sortase A mediated multi-enzyme assembly. The increase in activity (2.7-fold) was obtained with cage: Cel48S/ Cel8A than the mixture of singly modified cages (cage: Cel48S and cage: Cel8A) [70].

#### 4. Protein scaffolds employed in multi-enzyme assembly

There are numerous proteins present in nature that fascinatingly self-assemble into different nanostructures; mainly via protein-protein interactions. Due to current advancements in protein engineering, the self-assembly process could be controlled to create specifically designed protein scaffolds into precise supramolecular structures such as nanocages, filaments, rings, crystals, tubules, etc. [71]. From the last decade, researchers have designed various advanced nanobiocatalyst based on self-assembled protein scaffolds as a way to improve the stability and productivity of enzymes. Such protein nanocarriers and their effect on the kinetic parameters of the enzyme/s being immobilized are given in Table 2. In the following section, such nanobiocatalysts will be elaborated as per the type of protein scaffold used to either encapsulate enzymes in their interior or to display it on their exterior.

##### 4.1. Virus-like particles

Virus-like particles (VLPs) are non-infectious, self-assembling nanocages derived from discrete numbers of viral capsid proteins that resemble the overall structure of virus particles but are devoid of native viral machinery [81]. These VLPs are widely used as a nanoreactor where enzymes are encapsulated within the interior of VLPs. Encapsulation of enzymes within VLPs is a promising approach to mitigate enzyme degradation by protease attack, pH shifts, and high-temperature conditions. The ability to control the pore sizes of VLPs further improves the selectivity of enzymes as it facilitates selective entry and exit of

substrates and products. Another benefit of using VLPs is the compartmentalization of complex multi-enzyme cascades intended to simulate the multi-enzyme micro-compartments found in nature; for example, ethanolamine utilization micro-compartments [82]. Following are some examples of VLPs designed for enzyme encapsulation.

##### 4.1.1. Cowpea chlorotic mottle virus

Cowpea chlorotic mottle virus (CCMV) is a 28 nm icosahedral single-stranded RNA plant virus that belongs to the family of *Bromoviridae*. It is made up of 180 identical copies of coat proteins (CP) with T3 triangulation number that self-assembled into 20 hexamers and 12 pentamers. One of the appealing properties of CCMV is, an *in vitro* reversible self-assembly of CP. Additionally, the CCMV capsid shell is known to contain multiple pores of roughly 2 nm in size which allow diffusion [83]. These features make CCMV a suitable candidate for the production of a CCMV VLP based nanoreactor. With regards to this, CCMV capsid disassembles into dimers to release its RNA cargo at  $\text{pH} \geq 7.5$  and under higher ionic strength ( $\sim 1$  M). Consequently, RNA is removed by precipitation using calcium ions, and resultant CP dimers are re-assembled to form CCMV VLPs by lowering the pH towards 4.5 [84, 82].

Various strategies have been applied for the encapsulation of enzymes inside the CCMV VLPs. One study utilized the pH-dependent responsiveness of CCMV capsid to incorporate horseradish peroxidase within the capsid [85]. In another study, two different enzyme pairs *viz.*, GOx:DNAzymes and GOx:gluconokinase were encapsulated via non-covalent electrostatic interactions between negatively charged single-stranded DNA tagged enzymes and positively charged interior of capsid during the assembly process [83]. Furthermore, the Sortase A-mediated ligation strategy has also been used to demonstrate highly efficient cargo loading in CCMV VLPs wherein the polyglycine peptide is fused with N-terminal of CP and LPETG tag was fused to target protein followed by sortase A mediated isopeptide bond formation between them [86].

##### 4.1.2. P22

P22 bacteriophage is a temperate phage of *Salmonella typhimurium* that belongs to the *Podoviridae* family. The P22 capsid structure exhibit T7 triangulation number icosahedral symmetry consisting of 420 copies of 46.6 kDa CP that self assembles on to the approximately 100–330 copies of 33.6 kDa scaffolding protein (SP) through non-covalent interactions with C-terminus of SPs forming compact procapsid (PC) structure [87]. The PC structure is (58 nm diameter) double in size of CCMV VLPs and can form different capsid architecture with alterations in capsid porosity and internal volume by simply changing the incubation temperature and time of capsid formation. Heating at 60 °C for 15 min irreversibly changes the PC form to an expanded shell form (EX) with a doubling of the internal volume and increase in the diameter (60 nm) but with the loss of SPs. These two forms can be further transformed into wiffleball form (WB) by heating at 70 °C for 20 min. During the heating process, CP pentons dissociate from each of the five vertices in the EX capsid structure which leads to the formation of 10 nm of pores in the resulting WB VLPs with no change in the diameter [88]. All three morphologies of P22 VLPs allow researchers to easily modulate the porosity and internal volume of capsid to design a versatile nanoreactor.

Directed encapsulation of enzyme cascade involved in sugar metabolism within a P22 VLPs was reported which comprises  $\beta$ -glucosidase (CelB), ATP-dependent galactokinase (GALK), and ADP-dependent glucokinase (GLUK) [89]. This was achieved by constructing multi-enzyme fusion where two and three enzymes fused with each other and to the SP monomers through a polyglycine flexible linker, thus forming CelB-GLUK-SP and GALK-GLUK-CelB-SP complex respectively. SP monomer directs the entry of multi-enzyme fusions inside the P22 VLPs. In both these cases, enzyme kinetics of resulting CelB-GLUK-P22 and GALK-GLUK-CELB-P22 VLPs was improved significantly [89]. Besides this, another study of green fluorescent protein (GFP) and head domain of hemagglutinin protein from influenza (HAhead) was

**Table 2**  
Kinetic analysis of multi-enzyme assembly.

Protein carrier	Enzyme	Immobilization strategy	Kinetic parameters			
			Free enzyme	$V_{max}$ Immobilised enzyme	Free enzyme	$K_m$ Immobilised enzyme
Elastin-like polypeptide	MenD - enzyme involved in menaquinone biosynthesis.	SpyCatcher-SpyTag mediated covalent bonding	$\sim 2.7 \mu\text{M}\cdot\text{min}^{-1}$	Cyclic assembly: $5.0 \mu\text{M}\cdot\text{min}^{-1}$ ; Cross-linked assembly: $3.5 \mu\text{M}\cdot\text{min}^{-1}$	$32.9 \pm 1.7 \mu\text{M}$	Cyclic assembly: $32.9 \pm 3.0 \mu\text{M}$ ; Cross-linked assembly: $15.40 \pm 1.6 \mu\text{M}$
Ferritin Apo ferritin	$\alpha$ -amylase Glucose oxidase	EDC/NHS mediated cross-linking Streptavidin- biotin based non-covalent assembly	$10.6 \times 10^{-5} \text{U}\cdot\text{mg}^{-1}$ $0.05 \text{mM}\cdot\text{min}^{-1}\cdot\text{mg}^{-1}$	$3.3 \times 10^{-5} \text{U}\cdot\text{mg}^{-1}$ $0.51 \text{mM}\cdot\text{min}^{-1}\cdot\text{mg}^{-1}$	$2.63 \text{mg}\cdot\text{mL}^{-1}$ $9.95 \text{mM}\cdot\text{L}^{-1}$	$5.19 \text{mg}\cdot\text{mL}^{-1}$ $7.54 \text{mM}\cdot\text{L}^{-1}$
T4 phage capsid	Hoc fused amylase, maltase, and glucokinase	SpyCatcher-SpyTag mediated covalent bonding	Hoc-enzyme fusion mix: $6.31 \pm 0.12 \text{nM}\cdot\text{s}^{-1}$ ; Free enzyme mix: $4.33 \pm 1.21 \text{nM}\cdot\text{s}^{-1}$	$78.50 \pm 4.9 \text{nM}\cdot\text{s}^{-1}$	Hoc-enzyme fusion mix: $(3.00 \pm 0.71) \times 10^6 \text{nM}$ ; Free enzyme mix: $(3.77 \pm 1.59) \times 10^4 \text{nM}$	$(2.50 \pm 0.20) \times 10^6 \text{nM}$
Human ferritin H chain	$\beta$ -glucosidase	<i>E. coli</i> K coil and E coil interactions	$51.79 \text{s}^{-1}\cdot\text{mM}^{-1}$	$k_{cat}/K_m$ value: $48.99 \text{s}^{-1}\cdot\text{mM}^{-1}$	$1.26 \text{mM}$	$1.44 \text{mM}$
Twigged streptavidin polymer scaffold	Cellulase	Sortase A-based ligation	-	-	-	-
Synthetic protein	Triosephosphate isomerase, aldolase and fructose 1,6-bisphosphatase	Cohesin-dockerin based high affinity non-covalent interaction	Enzyme mixture: $2.39 \text{mM}^{-1}\cdot\text{min}^{-1}$	$k_{cat}/K_m$ value: $79.70 \text{mM}^{-1}\cdot\text{min}^{-1}$	Enzyme mixture: $1.63 \pm 0.28 \text{mM}$	$0.46 \pm 0.12 \text{mM}$
Synthetic protein	Lipase and p450 fatty acid decarboxylase	Cohesin -dockerin based high affinity non-covalent interaction	Enzyme mixture: $2.10 \times 10^4 \text{M}^{-1}\cdot\text{s}^{-1}$	$k_{cat}/K_m$ value: $1.30 \times 10^6 \text{M}^{-1}\cdot\text{s}^{-1}$	-	-
Interacting proteins- IPA/IPa, IPB/IPb, and IPC/IPC	Endoglucanase (EG), exoglucanase (CBH) and $\beta$ -glucosidase (BGL)	Glycine-serine linker mediated covalent bonding	-	-	Enzyme activity:	After a 4-h reaction, a 1.5-fold increase in enzyme activity for the tri-enzyme complex than corresponding free enzymes
SP1	Cellulase	Cohesin(Coh)-Dockerin (Doc) based high affinity non-covalent interaction	A cellulase constructs having a longer linker to its dockerin, termed Doc-1-cellulase.	-	-	-
EutM	Alcohol dehydrogenase (ADH)	SpyCatcher-SpyTag mediated covalent bonding	-	-	-	-
Gamma-prefoldin ( $\gamma$ -PFD)	Glucose oxidase (GOx) and horseradish peroxidase (HRP)	SpyCatcher-SpyTag mediated covalent bonding	-	-	HRP: $0.9 \pm 0.2 \times 10^{-3} \text{M}$ ; SpyCatcher-HRP: $1.0 \pm 0.2 \times 10^{-3} \text{M}$ ; GOx: $21 \pm 4 \times 10^{-3} \text{M}$ ; SpyCatcher-GOx: $21 \pm 2 \times 10^{-3} \text{M}$	SpyCatcher-HRP + $\gamma$ -PFD scaffold: $1.1 \pm 0.2 \times 10^{-3} \text{M}$ ; SpyCatcher-GOx + $\gamma$ -PFD scaffold: $18 + 2 \times 10^{-3} \text{M}$
Apo ferritin (Afftn)	GFP fused enzymes: human carbonic anhydrase (G-CA), (retro-) aldolase (RA-G) and Kemp eliminase (G-KE)	Encapsulation	G-CA: $(1.4 \pm 0.4) \times 10^3 \text{M}^{-1}\cdot\text{s}^{-1}$ ; RA-G: $(1.4 \pm 0.2) \times 10^4 \text{M}^{-1}\cdot\text{s}^{-1}$ ; G-KE: $(9.9 \pm 1.0) \times 10^4 \text{M}^{-1}\cdot\text{s}^{-1}$	$k_{cat}/K_m$ value: G-CA+ Afftn: $(1.2 \pm 0.3) \times 10^3 \text{M}^{-1}\cdot\text{s}^{-1}$ ; RA-G+ Afftn: $(2.2 \pm 0.2) \times 10^4 \text{M}^{-1}\cdot\text{s}^{-1}$ ; G-KE+ Afftn: $(11.2 \pm 2.5) \times 10^4 \text{M}^{-1}\cdot\text{s}^{-1}$	RA-G: $300 \pm 20 \mu\text{M}$ ; G-KE: $1700 \pm 200 \mu\text{M}$	RA-G+ Afftn: $280 \pm 30 \mu\text{M}$ ; G-KE+ Afftn: $1400 \pm 100 \mu\text{M}$

attempted to display on the exterior surface of CP of P22 VLPs via a sortase based ligation approach [88]. Results support an overall concept and modularity of the approach where LPTEG tagged P22 VLPs scaffold can be used for the display of multiple proteins of interest [88].

The catalytic activity of encapsulated ADH was finely tuned by controlling the stoichiometry of enzyme loading and packing density of enzymes inside the P22 VLPs [90]. Compositional control was achieved by mixing different ratios of ADH fused SP (ADH-SP) and wild type SPs (wtSPs) during *in vitro* assembly of P22 VLPs whereas packing density was controlled by selective removal of wtSPs through P22 capsid pores using mild treatment with a chaotrope. The wtSPs were observed to exert a crowding effect on the enzyme which finely tuned the enzymatic output [90]. A similar approach was used to synthesize complex proteinaceous hierarchical structures with P22 VLPs that mimic cellular

environments having different macromolecules and subcellular compartments [91]. As a proof of concept, the ferritin nanocage which acts as a separate confined compartment and  $\beta$ -glucosidase was co-encapsulated with a controlled stoichiometry of loading within P22 VLPs by fusion of the respective genes with SPs [91]. Altogether, the understanding gained from both the research could be useful to construct cell-like bioreactor for various biochemical reactions.

#### 4.2. Ferritin

Ferritin is an iron storage protein present in all domains of a life consisting of 24 identical monomers that self-assemble into a cage-like structure with 12 nm of outer diameter and 8 nm of inner diameter [92, 74]. Ferritin can store up to 4500 Fe(III) atoms having

Enzyme	Kinetic parameters				Reference
	$V_{max}$ Free enzyme	$K_m$ Free enzyme	Free enzyme	$k_{cat}$ Immobilised enzyme	
MenD - enzyme involved in menaquinone biosynthesis.	$\sim 2.7 \mu\text{M}\cdot\text{min}^{-1}$	$32.9 \pm 1.7 \mu\text{M}$	$1.45 \pm 0.03 \text{ min}^{-1}$	Cyclic assembly: $2.57 \pm 0.04 \text{ min}^{-1}$ ; Cross-linked assembly: $1.60 \pm 0.04 \text{ min}^{-1}$	[72]
$\alpha$ -amylase	$10.6 \times 10^{-5} \text{ U}\cdot\text{mg}^{-1}$	$2.63 \text{ mg}\cdot\text{mL}^{-1}$	-	-	[73]
Glucose oxidase	$0.05 \text{ mM}\cdot\text{min}^{-1}\cdot\text{mg}^{-1}$	$9.95 \text{ mM}\cdot\text{L}^{-1}$	-	-	[74]
Hoc fused amylase, maltase, and glucokinase	Hoc-enzyme fusion mix: $6.31 \pm 0.12 \text{ nM}\cdot\text{s}^{-1}$ ; Free enzyme mix: $4.33 \pm 1.21 \text{ nM}\cdot\text{s}^{-1}$	Hoc-enzyme fusion mix: $(3.00 \pm 0.71) \times 10^5 \text{ nM}$ ; Free enzyme mix: $(3.77 \pm 1.59) \times 10^4 \text{ nM}$	Hoc-enzyme fusion mix: $0.32 \pm 0.01 \text{ s}^{-1}$ ; Free enzyme mix: $0.87 \pm 0.24 \text{ s}^{-1}$	Retained activity at $50^\circ\text{C}$ : 50% for 1.5 h and 20% for 3 h 90% for 1.5 h and 50% for 3 h	[75]
$\beta$ -glucosidase	$k_{cat}/K_m$ value: $51.79 \text{ s}^{-1}\cdot\text{mM}^{-1}$	$1.26 \text{ mM}$	$65.26 \text{ s}^{-1}$	$70.55 \text{ s}^{-1}$	[26]
Cellulase	-	-	Amount of reducing sugar released: On PSC: $1.60 \text{ g}\cdot\text{L}^{-1}$ ; On avicel: $0.16 \text{ g}\cdot\text{L}^{-1}$		[61]
Triosephosphate isomerase, aldolase and fructose 1,6-bisphosphatase	$k_{cat}/K_m$ value: Enzyme mixture: $2.39 \text{ mM}^{-1}\cdot\text{min}^{-1}$	Enzyme mixture: $1.63 \pm 0.28 \text{ mM}$	Enzyme mixture: $3.90 \pm 0.29 \text{ min}^{-1}$	$36.30 \pm 2.90 \text{ min}^{-1}$	[76]
Lipase and p450 fatty acid decarboxylase	$k_{cat}/K_m$ value: Enzyme mixture: $2.10 \times 10^4 \text{ M}^{-1}\cdot\text{s}^{-1}$	-	Enzyme mixture: $0.17 \mu\text{M}\cdot\text{min}^{-1}$	Enzyme productivity: $4.60 \mu\text{M}\cdot\text{min}^{-1}$	[77]
Endoglucanase (EG), exoglucanase (CBH) and $\beta$ -glucosidase (BGL)	-	Enzyme activity: After a 4-h reaction, a 1.5-fold increase in enzyme activity for the tri-enzyme complex than corresponding free enzymes	BGL: $\sim 1.5 \text{ U}\cdot\mu\text{M}^{-1}$ ; CBH: $\sim 1.60 \text{ U}\cdot\mu\text{M}^{-1}$ ; EG: $\sim 1100 \text{ U}\cdot\mu\text{M}^{-1}$	Specific activity: BGL: $\sim 1.75 \text{ U}\cdot\mu\text{M}^{-1}$ ; CBH: $\sim 1.70 \text{ U}\cdot\mu\text{M}^{-1}$ ; EG: $\sim 820 \text{ U}\cdot\mu\text{M}^{-1}$	[78]
Cellulase	A cellulase constructs having a longer linker to its dockerin, termed Doc-L-cellulase.	-	Doc-cellulase: $9.0 \times 10^2 \text{ U}\cdot\mu\text{M}^{-1}$ ; Doc-L-cellulase: $4.3 \times 10^2 \text{ U}\cdot\mu\text{M}^{-1}$	Coh-SP1 + Doc-cellulase: $15.0 \times 10^2 \text{ U}\cdot\mu\text{M}^{-1}$ ; Coh-SP1 + Doc-L-cellulase: $8.5 \times 10^2 \text{ U}\cdot\mu\text{M}^{-1}$	[79]
Alcohol dehydrogenase (ADH)	-	-	ADH: $1100 \text{ mU}\cdot\text{mg}^{-1}$ ; SpyTag-ADH: $1500 \text{ mU}\cdot\text{mg}^{-1}$	Specific activity: 1.6 fold higher than SpyTag-ADH	[42]
Glucose oxidase (GOx) and horseradish peroxidase (HRP)	-	HRP: $0.9 \pm 0.2 \times 10^{-3} \text{ M}$ ; SpyCatcher-HRP: $1.0 \pm 0.2 \times 10^{-3} \text{ M}$ ; GOx: $21 \pm 4 \times 10^{-3} \text{ M}$ ; SpyCatcher-GOx: $21 \pm 2 \times 10^{-3} \text{ M}$	HRP: $2900 \pm 800 \text{ s}^{-1}$ ; SpyCatcher-HRP: $2400 \pm 500 \text{ s}^{-1}$ ; GOx: $160 \pm 30 \text{ s}^{-1}$ ; SpyCatcher-GOx: $150 \pm 20 \text{ s}^{-1}$	SpyCatcher-HRP + $\gamma$ -PFD scaffold: $4700 \pm 900 \text{ s}^{-1}$ ; SpyCatcher-GOx + $\gamma$ -PFD scaffold: $210 \pm 20 \text{ s}^{-1}$	[80]
GFP fused enzymes: human carbonic anhydrase (G-CA), (retro-)aldolase (RA-G) and Kemp eliminase (G-KE)	$k_{cat}/K_m$ value: G-CA: $(1.4 \pm 0.4) \times 10^3 \text{ M}^{-1}\cdot\text{s}^{-1}$ ; RA-G: $(1.4 \pm 0.2) \times 10^4 \text{ M}^{-1}\cdot\text{s}^{-1}$ ; G-KE: $(9.9 \pm 1.0) \times 10^4 \text{ M}^{-1}\cdot\text{s}^{-1}$	RA-G: $300 \pm 20 \mu\text{M}$ ; G-KE: $1700 \pm 200 \mu\text{M}$	RA-G: $4.3 \pm 0.1 \text{ s}^{-1}$ ; G-KE: $170 \pm 10 \text{ s}^{-1}$	RA-G + Afftn: $6.2 \pm 0.4 \text{ s}^{-1}$ ; G-KE + Afftn: $150 \pm 30 \text{ s}^{-1}$	[19]

paramagnetic properties which aid in easy recovery and reusability of scaffold system by an external magnetic field [73, 42]. It has wide pH and temperature stability. The pH-induced disassembly-reassembly process of apoferritin (ferritin cage without Fe(III) atoms) is pseudoreversible between a pH range of 10.00 to 2.66 [93]. Moreover, they are stable in various denaturants like sodium hydroxide, urea, and guanidinium chloride because of the presence of large numbers of salt bridges and hydrogen bonding between subunits [94]. Due to these marvelous properties ferritin has been used as a scaffold mainly in two different forms, viz; apoferritin and magnetoferritin.

Apoferritin has been used for the localization of enzymes such as GOx, aldolase, and  $\alpha$ -amylase [19, 73, 95]. Improved enzyme kinetics with a ten-fold increase in  $V_{max}$  and a 24% decrease in  $K_m$  values was observed when GOx was displayed on the apoferritin via streptavidin-biotin

interactions [95]. Furthermore, the stability of GOx was improved upon immobilization with a 1.8-fold and 2.5-fold increase in its retained activity for 1.5 h and 3 h respectively at  $50^\circ\text{C}$  than that of free GOx. This immobilized GOx was also stable at high (5 M) urea concentration with negligible loss of activity wherein the free GOx lost around 80% of its activity [95]. In another study, human carbonic anhydrase (G-CA), (retro-)aldolase (RA-G), and Kemp eliminase (G-KE) were encapsulated within an apoferritin cage individually via electrostatic interactions. This improved enzyme kinetics but the enzyme loading was very low (only 2–3 enzyme molecules per cage) [19]. This finding is consistent with the fact that apoferritin has a very tiny nanocage of 8 nm diameter which cannot accommodate more enzyme molecules; thus limiting the use of enzyme encapsulation strategy for the construction of ferritin-based nanobiocatalyst.

Yu Zhang et al. have used the magnetic properties of ferritin protein

to construct human H chain magnetoferritin based  $\beta$ -glucosidase enzyme complex that can be easily recovered from the reaction medium with an application of external magnetic fields [42]. This is a very promising approach that needs to explore because of its immense application in the development of robust recyclable industrial biocatalyst.

#### 4.3. SP1 protein

Stable protein 1 (SP1) isolated from *Populus tremula* aspen plant is a 148.8 kDa ring-like homo-dodecameric protein structure with an outer diameter of 11 nm and an inner core of 3 nm. This self-assembled protein is composed of 12 subunits that are held together via hydrophobic interactions and are expressed during adverse environmental stress such as cold, salinity, and heat stress in the plant [79]. It is noteworthy that SP1 protein is known to exert remarkable stability in boiling temperature with a melting temperature of 107 °C along with resistance to protease attack (trypsin, proteinase K and V8), organic solvents, and ionic detergent [96, 97]. SP1 protein has been engineered to construct artificial cellulosome where cohesin module was fused with SP1 monomer thus forming a Coh-SP1 fusion while dockerin module was linked to cellulase with and without linker peptide termed Doc-L-cellulase and Doc-cellulase respectively [79]. A long 23-residue linker was expected to prohibit a potential steric hindrance thereby ensuring proper folding and assembly of Coh-SP1 and dockerin bearing cellulase via cohesin-dockerin interactions. Though integration of peptide linker between cellulase and dockerin module enhances an enzyme loading capacity of Coh-SP1 scaffold, a two-fold decrease in specific activity of Doc-L-cellulase and their resultant scaffold complex was observed [79]. In another study, this Coh-SP1 protein scaffold was used to display exoglucanase where the synergistic effect of scaffolded exoglucanase and free endoglucanase was investigated using cellulose substrate. This combination was found to elevate the overall hydrolysis of cellulose by 20% [98].

#### 4.4. Shell protein of bacterial micro-compartments

Bacterial micro-compartments (BMC) are self-assembling semi-permeable multi-component protein compartments or organelle with a size in a range of 40–600 nm found in bacteria. It encapsulates a variety of enzyme cascades involved in anabolic (eg. carboxysome) or catabolic metabolism (eg. ethanolamine utilization BMC, propanediol utilization BMC) where protein shell provides an interface with cytosol [99]. The shell of BMC is made up of three types of structural proteins, each having one or two domain sequences of either Pfam00936 (that form cyclic homo-hexamers or pseudo-hexamers) or Pfam03319 (that form cyclic homopentamers) to function as hexagonal facets and pentagonal vertices of the BMC structure [100, 99].

The self-assembling nature of the shell proteins further potentiates the bottom-up bioengineering perspective to develop the synthetic BMC nanofactories which could encapsulate diverse compounds viz; non-endogenous cargo proteins, drug compounds, and enzyme cascades [101]. For instance, 1,2- propanediol (POD) utilization BMCs from *Salmonella enterica* was heterologously expressed in *E. coli* with the co-expression of  $\beta$ -galactosidase, esterase, and cofactor dependent glycerol dehydrogenase. These enzymes were fused with encapsulation peptide via a flexible glycine-rich linker for *in vivo* directed assembly within BMCs. Notably, the enzyme activity of all three enzymes was retained significantly whereas additional protection against acidic pH was observed due to BMC shell [101]. However, the use of encapsulation peptides often leads to aggregation of enzymes and hence has low

encapsulation efficiency. This issue has been circumvented by utilizing more specific strategies of enzyme-protein conjugation which would allow both *in vivo* and *in vitro* assembly of enzymes or cargo covalently on the surface of BMCs or within the core of BMCs [102, 103, 104, 42].

#### 4.5. PFD filament protein

Prefoldins (PFD) are the family of molecular chaperones found in both archaea and eukaryotes where they assist accurate protein folding in an ATP-independent manner. It is a hetero-hexameric complex consisting of six different subunits (in eukaryotes) and two  $\alpha$  and four  $\beta$  subunits (in archaea). For instance, gamma-prefoldin ( $\gamma$ -PFD), a filamentous chaperone protein isolated from *Methanocaldococcus janaschii* archaean found in deep-sea hydrothermal vents. This  $\gamma$ -PFD can self-assemble by forming a dimer of monomers followed by subsequent oligomerization of dimers through  $\beta$  bundle formation thus forming a filamentous structure of average length around 127 nm [105]. This filamentous chaperone exhibits high thermal stability with a melting temperature ( $T_m$ ) of 93 °C and stabilizes the other proteins from denaturation under unfavorable conditions [106]. All these features make them an ideal candidate for the controlled assembly of enzyme cascades.

Lim et al. have developed a versatile  $\gamma$ -PFD based scaffold system using SpyCatcher-SpyTag interaction domains that could scaffold a variety of enzymes or proteins of interest. The controlled immobilization of proteins on the scaffold was demonstrated using mCerulean3 and mVenus fluorescent protein. The impact of scaffolding on the catalytic activity was analyzed using horseradish peroxidase (HP) and GOx. The kinetic analysis revealed that the  $K_{cat}$  values of GOx-SpyCatcher and HP-SpyCatcher markedly increased upon localization on  $\gamma$ -PFD-SpyTag. On the contrary to this, colocalization of both the enzymes together on the  $\gamma$ -PFD-SpyTag scaffold did not further enhance sequential reaction, indicating no significant channeling of intermediates between the enzymes [80].

#### 4.6. Casein

Casein is a type of phosphoprotein consisting of four types of peptides:  $\alpha$ S1,  $\alpha$ S2,  $\beta$ - and  $\kappa$ -casein (in case of bovine milk) that differs in amino acid composition but have similar amphiphilic nature. These mixed, as well as pure forms of peptide, can self-assemble into micelles of around 50–500 nm in an aqueous solution. This self-assembly is pH and temperature-driven thus making it possible to encapsulate a variety of active molecules [107]. Furthermore, transglutaminase-aided cross-linking of casein with protein of interest forms a biopolymer that is applied for enzyme assembly [108].

There is only one study of this application where an artificial cellulosome was constructed using  $\beta$ -casein and N,N-dimethyl casein (DM-casein) as a scaffold [109]. Casein consists of 20 glutamine (Q) and 12 lysine (K) residues which are highly reactive substrates for microbial transglutaminase (MTG). MTG catalyzes acyl transfer reaction where  $\gamma$ -carboxamide groups of Q residues in the casein protein acts as the acyl donor while  $\epsilon$ -amino groups of K residues act as the acyl acceptor. This leads to the formation of  $\epsilon$ -( $\gamma$ -glutamyl)-lysine cross-linking within the protein of interest [110]. Therefore, this strategy has been utilized for the casein-enzyme conjugation where lysine-rich peptide sequence was fused with C-terminus of endoglucanase EG(Cel5A) and EG(Cel6A). Lysine residues of EG(Cel5A) and EG(Cel6A) undergo MTG mediated cross-linking with glutamine residues of  $\beta$ -casein and DM-casein forming casein-EG conjugate.  $\beta$ -casein also undergoes MTG-catalyzed self-cross-linking due to the presence of intrinsic reactive lysine residues but

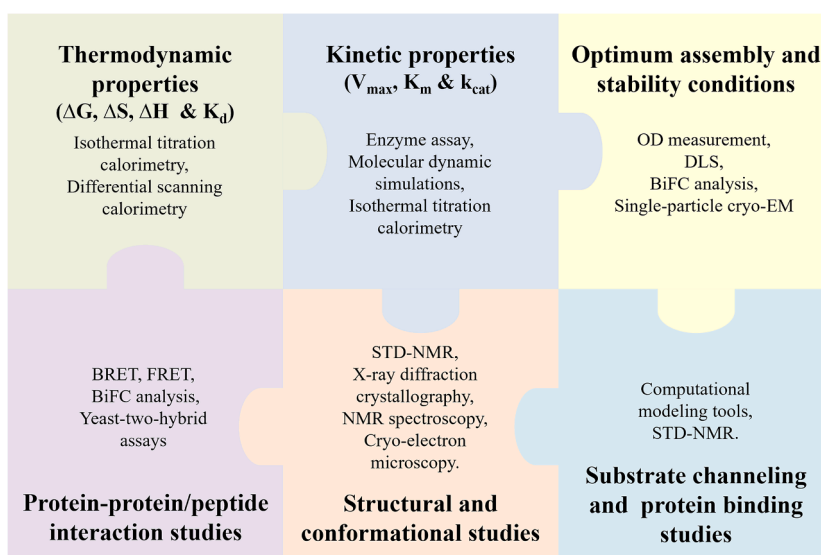


**Fig. 3.** Characterization Techniques for multi-enzyme complexes. (BiFC- bimolecular fluorescence complementation; BRET- bioluminescence resonance energy transfer analysis; FRET- fluorescence resonance energy transfer analysis; NMR- nuclear magnetic resonance; STD-NMR- saturation transfer difference NMR; cryo-EM- cryogenic electron microscopy).

this could hinder the processivity of the enzyme in the conjugate [109]. Though, DM-casein couldn't undergo self cross-linking by MTG due to the presence of modified lysine residues; it can facilitate control over enzyme loading per DM-casein. Cellulose saccharification with EG-DM-casein conjugate showed a two-fold increase as compared to EG- $\beta$ -casein conjugate enzyme: scaffold ratios were 1:6 [109]. The casein-based enzyme conjugates can be easily recovered from the reaction mixture by calcium-mediated precipitation. Hence, there is a great potential to explore and utilize the property of casein to improve the processivity of enzymes.

#### 4.7. Amyloid like nanofibrils

Amyloid nanofibrils are straight, unbranched, ubiquitous peptide/protein fibrous structures that are formed by the nucleation process. It is initiated with the self-assembly of soluble amyloidogenic peptides or proteins to form protofibrils onto which several other amyloidogenic peptides or proteins aggregate in highly ordered  $\beta$  sheet structures giving rise to a mature amyloid fiber [111]. Amyloid fibrils are generally 6–12 nm in diameter and few micrometers in length. These amyloid nanofibrils exist in two forms viz; nontoxic form essential for biological functions and disease-associated toxic form [111, 112].

There are few reports available on scaffolding the enzymatic cascades on nontoxic protein nanofibrils [113, 114]. One such example is where Sup35 amyloidogenic peptides were fused with xylanase A (XylA),  $\beta$ -xylosidase II ( $\beta$ -xyl), and aldose sugar dehydrogenase (ASD) to form three enzymatically functionalized fibrils for the production of xylonolactone [114]. The catalytic activity of enzymes was found to be unaffected in single enzyme-containing fibrils. Since there are differences in pH optima of the hemicellulases (pH 6.5) (XylA and  $\beta$ -xyl) and ASD pH (9.0), an 11-fold decrease in yield was obtained from the biocatalytic reaction at pH 7.5. To circumvent this issue, the author applied another strategy where xylose produced from XylA/ $\beta$ -xyl fibril complex was directly used as a substrate for ASD fibril complex at pH 9.0. This strategy was found to be more productive than immobilizing all three enzymes together on fibrils [114].

#### 5. Characterization of protein scaffold-based enzyme assembly

The strategies for the multi-enzyme assembly such as direct fusions, cross-linking and scaffold mediated assembly, may suffer from non-specific interactions during *in vivo/in vitro* assembly process which affects the overall processivity and stability of assembled enzymes. Hence, a study of enzyme binding parameters is crucial for understanding the entire process of multi-enzyme assembly. For this, exploring thermodynamic as well as kinetic properties of the multi-enzyme complex is of utmost importance (Fig. 3). An isothermal titration calorimetry is a major tool for thermodynamic characterization that investigates the types of interactions (hydrophobic, hydrophilic, electrostatic, polar, or non-polar) between the enzyme and scaffold. This is achieved by calculating the enthalpy ( $\Delta H$ ), entropy ( $\Delta S$ ), Gibbs free energy ( $\Delta G$ ), reaction stoichiometry ( $n$ ), and binding constant ( $K_D$ ) of the reaction simply by measuring the heat absorbed or evolved during the binding process [115]. Yet another tool named differential scanning calorimetry (DSC), a non-perturbing technique that can measure the molar heat capacity, phase transitions, conformational changes, and enthalpy changes. Molar heat capacity is directly used to investigate all the thermodynamic properties [116]. DSC-based thermal protein denaturation study provides information about the forces involved in the protein's conformational stability as well as the protein's unfolding process. The protein folding process can also be analyzed by measuring thermotropic changes in different reaction states [117]. It has been found that apart from enzymatic assay, enzyme kinetics can also be investigated using isothermal titration calorimetry [118, 119].

However, several authors have used optical density measurement ( $OD_{600}$ ) as the simplest approach to characterize turbidity which is indicative of the multi-enzyme complex formation under different reaction conditions [120, 121]. Dynamic light scattering (DLS), a non-invasive technique has been used for the determination of the particle size of the protein complexes which are in the range of 0.001  $\mu\text{m}$  to several microns. The thermal stability of the protein complex can also be assessed by using this tool as proteins denature under the influence of heat causing massive aggregation of denatured proteins which subsequently results in a significant increase in size and scattering intensity

[122]. Similarly, protein stability in different pH and concentrations can also be explored using DLS [123]. It has also been used for detecting assembly & disassembly processes of supramolecular structure [124, 120]. Furthermore, the overall binding mechanism, kinetics of the assembly process, and the conformational changes that occur during interactions can be studied using a molecular dynamics simulation approach [125, 126].

The protein-protein interactions during the assembly process can also be explored *in vivo* using conventional methods such as immunoprecipitation assay, bioluminescence resonance energy transfer (BRET) analysis, fluorescence resonance energy transfer (FRET) analysis, bimolecular fluorescence complementation (BiFC) analysis, and yeast-two-hybrid assays [127]. Recently, BiFC analysis is more widely accepted due to its advantages over other methods. BiFC analysis has been reported to study *in vivo* target protein interactions and their localization. Moreover, it is also been used to monitor the assembly-disassembly process of multi-enzyme complexes [128, 120].

Furthermore, the structural and functional analyses of multi-enzyme complexes are also crucial for investigating the processivity of enzyme components of the system as well as to get better mechanistic insights. Saturation transfer difference-nuclear magnetic resonance study (STD-NMR) has been reported to be used for identifying potential binding hotspots on the protein scaffold where different molecules can bind [129]. X-ray diffraction crystallography is a well-established method for structural analysis of proteins at atomic resolution [130]. Besides NMR and X-ray crystallography, for the past two decades, Single-particle Cryo-electron microscopy is gradually gaining popularity since unlike NMR and X-ray crystallography, it has the potential to visualize large, multi-subunit supramolecular complex without the requirement for a large volume of sample or crystallization. Luque and Castón have made an elaborated report on the use of Cryo-electron microscopy (Cryo-EM) to study dynamic processes of viral assembly using distinct conditions [131]. It could also reveal the information about substrate channeling within a multi-enzyme complex along with depicting the 3D structure of the complex [132, 133]. Computational modeling tools such as steered molecular dynamics simulation and molecular dynamic simulation along with binding energy calculations have been used to obtain mechanistic insights into the processivity of enzymes of the multi-enzyme complex [134].

Altogether, the above-described strategies, as well as examples of scaffold proteins, have gained popularity in the field of synthetic biology since such kinds of multi-enzyme systems not only improve overall fundamental understanding but also expand their applications as a cell-free system which would mimic the naturally occurring metabolic channeling processes.

## 6. Conclusion

The spatial organization of enzymatic cascades on suitable protein scaffold has rapidly gained attention as it resembles cellular multi-enzyme complexes where scaffolding plays an important role in substrate channeling to attain optimum catalytic efficiency and providing a stable microenvironment. Therefore, the natural concept of scaffolding enzyme cascades has been adapted with the integration of synthetic biology for the development of an artificial scaffold system. With regards to this, diverse proteins have been utilized for creating artificial scaffold systems based on their remarkable properties. Their results signify that promising progress in this field has been made. However, further investigation is requisite for designing scaffold systems for complex metabolic pathways as well as for optimization of the system

for large-scale industrial applications. This will create more robust mega-enzyme assemblies which will broaden its applications in the field of biofuel and bioprocess technology, enzyme engineering, and biosensor.

## CRedit authorship contribution statement

**Shubhada Gad:** Formal analysis, Writing – original draft. **Sonal Ayakar:** Writing – review & editing, Writing – original draft, Supervision.

## Declaration of Competing Interest

The authors declare that they have no known competing financial interests or personal relationships that could have appeared to influence the work reported in this paper.

## References

- [1] C.L. Kohnhorst, M. Kyoung, M. Jeon, D.L. Schmitt, E.L. Kennedy, J. Ramirez, S. An, Identification of a multi-enzyme complex for glucose metabolism in living cells, *J. Biol. Chem.* 292 (22) (2017) 9191–9203, <https://doi.org/10.1074/jbc.M117.783050>.
- [2] J. Kim, J.W. Grate, P. Wang, Nanobiocatalysis and its potential applications, *Trends Biotechnol.* 26 (11) (2008) 639–646, <https://doi.org/10.1016/j.tibtech.2008.07.009>.
- [3] S. Asmat, A.H. Anwer, Q. Husain, Immobilization of lipase onto novel constructed polydopamine grafted multiwalled carbon nanotube impregnated with magnetic cobalt and its application in synthesis of fruit flavours, *Int. J. Biol. Macromol.* 140 (2019) 484–495, <https://doi.org/10.1016/j.ijbiomac.2019.08.086>.
- [4] C.M. Fung, J.S. Lloyd, S. Samavat, D. Deganello, K.S. Teng, Facile fabrication of electrochemical ZnO nanowire glucose biosensor using roll to roll printing technique, *Sensors and Actuators, B: Chem.* 247 (2017) 807–813, <https://doi.org/10.1016/j.snb.2017.03.105>.
- [5] Y. Wang, D. Chen, G. Wang, C. Zhao, Y. Ma, W. Yang, Immobilization of cellulase on styrene/maleic anhydride copolymer nanoparticles with improved stability against pH changes, *Chem. Eng. J.* 336 (2018) 152–159, <https://doi.org/10.1016/j.cej.2017.11.030>.
- [6] B. Boscolo, F. Trotta, E. Ghibaudi, High catalytic performances of *Pseudomonas fluorescens* lipase adsorbed on a new type of cyclodextrin-based nanospheres, *J. Mol. Catalysis B: Enzymatic* 62 (2) (2010) 155–161, <https://doi.org/10.1016/j.molcatb.2009.10.002>.
- [7] P. Wu, F. Luo, Z. Lu, Z. Zhan, G. Zhang, Improving the catalytic performance of pectate lyase through pectate lyase/Cu<sub>3</sub>(PO<sub>4</sub>)<sub>2</sub> hybrid nanoflowers as an immobilized enzyme, *Front. Bioeng. Biotechnol.* 8 (2020) 280, <https://doi.org/10.3389/fbioe.2020.00280>.
- [8] C. Lin, K. Xu, R. Zheng, Y. Zheng, Immobilization of amidase into a magnetic hierarchically porous metal-organic framework for efficient biocatalysis, *Chem. Commun.* 55 (40) (2019) 5697–5700, <https://doi.org/10.1039/c9cc02038a>.
- [9] Silva-Torres, O., Bojorquez-Vazquez, L., Simakov, A., & Vazquez-Duhalt, R. (2019). Enhanced laccase activity of biocatalytic hybrid copper hydroxide nanocages. *Enzyme and microbial technology*, 128, 59–66. [10.1016/j.enzmictec.2019.05.008](https://doi.org/10.1016/j.enzmictec.2019.05.008).
- [10] A. Uzunoglu, The use of CeO<sub>2</sub>-TiO<sub>2</sub> nanocomposites as enzyme immobilization platforms in electrochemical sensors, *J. Turkish Chem. Society, Section A: Chem.* 4 (3) (2017) 855–868, <https://doi.org/10.18596/jotcsa.327686>.
- [11] C. Blanchette, C.I. Lacayo, N.O. Fischer, M. Hwang, M.P. Thelen, Enhanced cellulose degradation using cellulase-nanosphere complexes, *PLoS ONE* 7 (8) (2012) e42116, <https://doi.org/10.1371/journal.pone.0042116>.
- [12] I.N. Ahmed, X.L. Yang, A.A. Dubale, R.F. Li, Y.M. Ma, L.M. Wang, M.H. Xie, Hydrolysis of cellulose using cellulase physically immobilized on highly stable zirconium based metal-organic frameworks, *Bioresour. Technol.* 270 (2018) 377–382, <https://doi.org/10.1016/j.biortech.2018.09.077>.
- [13] U.V. Sojitra, S.S. Nadar, V.K. Rathod, Immobilization of pectinase onto chitosan magnetic nanoparticles by macromolecular cross-linker, *Carbohydr. Polym.* 157 (2017) 677–685, <https://doi.org/10.1016/j.carbpol.2016.10.018>.
- [14] Y. Rui, X. Wu, B. Ma, Y. Xu, Immobilization of acetylcholinesterase on functionalized SBA-15 mesoporous molecular sieve for detection of organophosphorus and carbamate pesticide, *Chinese Chem. Lett.* 29 (9) (2018) 1387–1390, <https://doi.org/10.1016/j.ccl.2017.10.033>.
- [15] R. Li, J. Yang, Y. Xiao, L. Long, *In vivo* immobilization of an organophosphorus hydrolyzing enzyme on bacterial polyhydroxyalkanoate nano-granules, *Microb. Cell Fact.* 18 (1) (2019) 1–10, <https://doi.org/10.1186/s12934-019-1201-2>.

- [16] F. Mickoleit, D. Schüler, Generation of multifunctional magnetic nanoparticles with amplified catalytic activities by genetic expression of enzyme arrays on bacterial magnetosomes, *Adv. Biosyst.* 2 (1) (2018), 1700109, <https://doi.org/10.1002/adbi.201700109>.
- [17] O. González-Davis, K. Chauhan, S.J. Zapian-Merino, R. Vazquez-Duhalt, Bi-enzymatic virus-like bionanoreactors for the transformation of endocrine disruptor compounds, *Int. J. Biol. Macromol.* 146 (2020) 415–421, <https://doi.org/10.1016/j.ijbiomac.2019.12.272>.
- [18] F. Visser, B. Müller, J. Rose, D. Prüfer, G.A. Noll, Forzymes-functionalised artificial forisomes as a platform for the production and immobilisation of single enzymes and multi-enzyme complexes, *Sci Rep* 6 (1) (2016) 1–15, <https://doi.org/10.1038/srep30839>.
- [19] S. Tetter, D. Hilvert, Enzyme encapsulation by a ferritin cage, *Angewandte Chemie Int. Ed.* 56 (47) (2017) 14933–14936, <https://doi.org/10.1002/anie.201708530>.
- [20] C.J. Delebecque, A.B. Lindner, P.A. Silver, F.A. Aldaye, Organization of intracellular reactions with rationally designed RNA assemblies, *Science* 333 (2011) 470–474, <https://doi.org/10.1126/science.1206938>.
- [21] J. Fu, M. Liu, Y. Liu, N.W. Woodbury, H. Yan, Interenzyme substrate diffusion for an enzyme cascade organized on spatially addressable DNA nanostructures, *J. Am. Chem. Soc.* 134 (12) (2012) 5516–5519, <https://doi.org/10.1021/ja300897h>.
- [22] O.I. Wilner, S. Shimron, Y. Weizmann, Z.G. Wang, I. Willner, Self-assembly of enzymes on dna scaffolds: en route to biocatalytic cascades and the synthesis of metallic nanowires, *Nano Lett.* 9 (5) (2009) 2040–2043, <https://doi.org/10.1021/nl900302z>.
- [23] A.V. Pinheiro, D. Han, W.M. Shih, H. Yan, Challenges and opportunities for structural DNA nanotechnology, *Nat. Nanotechnol.* 6 (12) (2011) 763–772, <https://doi.org/10.1038/nnano.2011.187>.
- [24] R. Chen, Q. Chen, H. Kim, K.H. Siu, Q. Sun, S.L. Tsai, W. Chen, Biomolecular scaffolds for enhanced signaling and catalytic efficiency, *Curr. Opin. Biotechnol.* 28 (2014) 59–68, <https://doi.org/10.1016/j.copbio.2013.11.007>.
- [25] P. Rapali, R. Mitteau, C. Braun, A. Massoni-Laporte, C. Ünlü, L. Bataille, D. McCusker, Scaffold-mediated gating of Cdc42 signalling flux, *Elife* 6 (2017) e25257, <https://doi.org/10.7554/eLife.25257>.
- [26] Y. Zhang, Y. Dong, J. Zhou, Y. Hu, X. Li, F. Wang, Peptide-mediated immobilization on magnetoferritin for enzyme recycling, *Nanomaterials* 9 (11) (2019) 1558, <https://doi.org/10.3390/nano9111558>.
- [27] J.E. Dueber, G.C. Wu, G.R. Malmirchegini, T.S. Moon, C.J. Petzold, A.V. Ullal, J. D. ...Keasling, Synthetic protein scaffolds provide modular control over metabolic flux, *Nat. Biotechnol.* 27 (8) (2009) 753–759, <https://doi.org/10.1038/nbt.1557>.
- [28] S. Hezaveh, A.P. Zeng, U. Jandt, Human pyruvate dehydrogenase complex E2 and E3BP core subunits: new models and insights from molecular dynamics simulations, *J. Phys. Chem. B* 120 (19) (2016) 4399–4409, <https://doi.org/10.1021/acs.jpcc.6b02698>.
- [29] S. Morais, J. Stern, A. Kahn, A.P. Galanopoulou, S. Yoav, M. Shamshoum, E. A. Bayer, Enhancement of cellulose-mediated deconstruction of cellulose by improving enzyme thermostability, *Biofuels* 9 (1) (2016) 1–12, <https://doi.org/10.1186/s13068-016-0577-z>.
- [30] B.Bin Hu, M.J. Zhu, Reconstitution of cellulosome: research progress and its application in biorefinery, *Biotechnol. Appl. Biochem.* 66 (5) (2019) 720–730, <https://doi.org/10.1002/bab.1804>.
- [31] C.J. Chiang, L.J. Lin, Z.W. Wang, T.T. Lee, Y.P. Chao, Design of a noncovalently linked bifunctional enzyme for whole-cell biotransformation, *Process Biochem.* 49 (7) (2014) 1122–1128, <https://doi.org/10.1016/j.procbio.2014.03.016>.
- [32] F. Liu, S. Banta, W. Chen, Functional assembly of a multi-enzyme methanol oxidation cascade on a surface-displayed trifunctional scaffold for enhanced NADH production, *Chem. Commun.* 49 (36) (2013) 3766–3768, <https://doi.org/10.1039/c3cc40454d>.
- [33] R.P. Bhattacharyya, A. Reményi, B.J. Yeh, W.A. Lim, Domains, motifs, and scaffolds: the role of modular interactions in the evolution and wiring of cell signaling circuits, *Annu. Rev. Biochem.* 75 (1) (2006) 655–680, <https://doi.org/10.1146/annurev.biochem.75.103004.142710>.
- [34] M.J. Wagner, M.M. Stacey, B.A. Liu, T. Pawson, Molecular mechanisms of SH2- and PTB-Domain-containing proteins in receptor tyrosine kinase signaling, *Cold Spring Harb. Perspect. Biol.* 5 (12) (2013) 1–19, <https://doi.org/10.1101/cshperspect.a008987>.
- [35] Y. Barak, T. Handelsman, D. Nakar, A. Mechaly, R. Lamed, Y. Shoham, E.A. Bayer, Matching fusion protein systems for affinity analysis of two interacting families of proteins: the cohesin-dockerin interaction, *J. Mol. Recognit.* 18 (6) (2005) 491–501, <https://doi.org/10.1002/jmr.749>.
- [36] A. Peer, S.P. Smith, E.A. Bayer, R. Lamed, I. Borovok, Noncellulosomalcohesin- and dockerin-like modules in the three domains of life, *FEMS Microbiol. Lett.* 291 (1) (2009) 1–16, <https://doi.org/10.1111/j.1574-6968.2008.01420.x>.
- [37] J.J. Adams, B.A. Webb, H.L. Spencer, S.P. Smith, Structural characterization of type II dockerin module from the cellulosome of *Clostridium thermocellum*: calcium-induced effects on conformation and target recognition, *Biochemistry* 44 (6) (2005) 2173–2182, <https://doi.org/10.1021/bi048039u>.
- [38] A. Karpol, L. Kantorovich, A. Demishten, Y. Barak, E. Morag, R. Lamed, E. A. Bayer, Engineering a reversible, high-affinity system for efficient protein purification based on the cohesin-dockerin interaction, *J. Mol. Recognition: An Interdisciplinary J.* 22 (2) (2009) 91–98, <https://doi.org/10.1002/jmr.926>.
- [39] S. Kim, J.S. Hahn, Synthetic scaffold based on a cohesin-dockerin interaction for improved production of 2, 3-butanediol in *Saccharomyces cerevisiae*, *J. Biotechnol.* 192 (2014) 192–196, <https://doi.org/10.1016/j.jbiotec.2014.10.015>.
- [40] L. Chen, A. Mulchandani, X. Ge, Spore-displayed enzyme cascade with tunable stoichiometry, *Biotechnol. Prog.* 33 (2) (2017) 383–389, <https://doi.org/10.1002/btpr.2416>.
- [41] A.H. Keeble, M. Howarth, Insider information on successful covalent protein coupling with help from SpyBank, *Meth. Enzymol.* 617 (2019) 443–461, <https://doi.org/10.1016/bs.mie.2018.12.010>.
- [42] G. Zhang, T. Johnston, M.B. Quin, C. Schmidt-Dannert, Developing a protein scaffolding system for rapid enzyme immobilization and optimization of enzyme functions for biocatalysis, *ACS Synth. Biol.* 8 (8) (2019) 1867–1876, <https://doi.org/10.1021/acssynbio.9b00187>.
- [43] D. Hatlem, T. Trunk, D. Linke, J.C. Leo, Catching a SPY: using the SpyCatcher-SpyTag and related systems for labeling and localizing bacterial proteins, *Int. J. Mol. Sci.* 20 (9) (2019) 2129, <https://doi.org/10.3390/ijms20092129>.
- [44] B. Zakeri, J.O. Fierer, E. Celik, E.C. Chittock, U. Schwarz-Linek, V.T. Moy, M. Howarth, Peptide tag forming a rapid covalent bond to a protein, through engineering a bacterial adhesin, *Proceedings of the National Academy of Sciences* 109 (12) (2012) E690–E697, <https://doi.org/10.1073/pnas.1115485109>.
- [45] L. Jia, K. Minamihata, H. Ichinose, K. Tsumoto, N. Kamiya, Polymeric SpyCatcher Scaffold enables bioconjugation in a ratio-controllable manner, *Biotechnol. J.* 12 (12) (2017), 1700195, <https://doi.org/10.1002/biot.201700195>.
- [46] Y. Lin, W. Jin, J. Wang, Z. Cai, S. Wu, G. Zhang, A novel method for simultaneous purification and immobilization of a xylanase-lichenase chimera via SpyTag/SpyCatcher spontaneous reaction, *Enzyme Microb. Technol.* 115 (2018) 29–36, <https://doi.org/10.1016/j.enzmictec.2018.04.007>.
- [47] D. Dovala, W.S. Sawyer, C.M. Rath, L.E. Metzger, Rapid analysis of protein expression and solubility with the SpyTag-SpyCatcher system, *Protein Expr. Purif.* 117 (2016) 44–51, <https://doi.org/10.1016/j.pep.2015.09.021>.
- [48] F.S. Aalbers, M.W. Fraaije, Enzyme fusions in biocatalysis: coupling reactions by pairing enzymes, *Chem. Bio. Chem.* 20 (1) (2019) 20–28, <https://doi.org/10.1002/cbic.201800394>.
- [49] T. Haga, H. Hirakawa, T. Nagamune, Fine tuning of spatial arrangement of enzymes in a PCNA-mediated multi-enzyme complex using a rigid poly-L-proline linker, *PLoS ONE* 8 (9) (2013) 1–11, <https://doi.org/10.1371/journal.pone.0075114>.
- [50] Y. Zhang, Y. Wang, S. Wang, B. Fang, Engineering bi-functional enzyme complex of formate dehydrogenase and leucine dehydrogenase by peptide linker mediated fusion for accelerating cofactor regeneration, *Eng. Life Sci.* 17 (9) (2017) 989–996, <https://doi.org/10.1002/elsc.201600232>.
- [51] S.Y. Tsujii, D.E. Cane, C. Khosla, Selective protein-protein interactions direct channeling of intermediates between polyketide synthase modules, *Biochemistry* 40 (8) (2001) 2326–2331, <https://doi.org/10.1021/bi002463n>.
- [52] H. Wang, J. Liang, Q. Yue, L. Li, Y. Shi, G. Chen, X. Ding, Engineering the acyltransferase domain of epothilone polyketide synthase to alter the substrate specificity, *Microb. Cell Fact.* 20 (1) (2021) 1–14, <https://doi.org/10.1186/s12934-021-01578-3>.
- [53] C.J. Hartley, C.C. Williams, J.A. Scoble, Q.I. Churches, A. North, N.G. French, C. Scott, Engineered enzymes that retain and regenerate their cofactors enable continuous-flow biocatalysis, *Nat. Catalysis* 2 (11) (2019) 1006–1015, <https://doi.org/10.1038/s41929-019-0353-0>.
- [54] Á. Mourelle-Insua, F.S. Aalbers, I. Lavandera, V. Gotor-Fernández, M.W. Fraaije, What to sacrifice? Fusions of cofactor regenerating enzymes with Baeyer-Villiger monooxygenases and alcohol dehydrogenases for self-sufficient redox biocatalysis, *Tetrahedron* 75 (13) (2019) 1832–1839, <https://doi.org/10.1016/j.tet.2019.02.015>.
- [55] P.Å. Nygren, Alternative binding proteins: affibody binding proteins developed from a small three-helix bundle scaffold, *FEBS J.* 275 (11) (2008) 2668–2676, <https://doi.org/10.1111/j.1742-4658.2008.06438.x>.
- [56] M. Lindborg, A. Dubnovitsky, K. Olesen, T. Björkman, L. Abrahmsén, J. Feldwisch, T. Härd, High-affinity binding to staphylococcal protein A by an engineered dimeric Affibody molecule, *Protein Eng. Des. Selection*, 26 (10) (2013) 635–644, <https://doi.org/10.1093/protein/gzt038>.
- [57] J. Löfblom, J. Feldwisch, V. Tolmachev, J. Carlsson, S. Ståhl, F.Y. Frejd, Affibody molecules: engineered proteins for therapeutic, diagnostic and biotechnological applications, *FEBS Lett.* 584 (12) (2010) 2670–2680, <https://doi.org/10.1016/j.febslet.2010.04.014>.
- [58] M. Eklund, L. Axelsson, M. Uhlén, P.Å. Nygren, Anti-idiotypic protein domains selected from protein A-based affibody libraries, *Proteins: Struct., Funct. Genet.*, 48 (3) (2002) 454–462, <https://doi.org/10.1002/prot.10169>.
- [59] S. Tippmann, J. Anfelt, F. David, J.M. Rand, V. Siewers, M. Uhlén, E.P. Hudson, Affibody scaffolds improve sesquiterpene production in *Saccharomyces*

- cerevisiae, *ACS Synth. Biol.* 6 (1) (2017) 19–28, <https://doi.org/10.1021/acssynbio.6b00109>.
- [60] M. Eklund, K. Sandström, T.T. Teeri, P.Å. Nygren, Site-specific and reversible anchoring of active proteins onto cellulose using a cellulosome-like complex, *J. Biotechnol.* 109 (3) (2004) 277–286, <https://doi.org/10.1016/j.jbiotec.2004.01.008>.
- [61] T. Matsumoto, Y. Isogawa, K. Minamihata, T. Tanaka, A. Kondo, Twiggged streptavidin polymer as a scaffold for protein assembly, *J. Biotechnol.* 225 (2016) 61–66, <https://doi.org/10.1016/j.jbiotec.2016.03.030>.
- [62] A.W. Jacobitz, M.D. Kattke, J. Wereszczynski, R.T. Clubb, Sortase transpeptidases: structural biology and catalytic mechanism, *Adv. Protein Chem. Struct. Biol.* 109 (2017) 223–264, <https://doi.org/10.1016/bs.apcsb.2017.04.008>.
- [63] X. Dai, A. Böker, U. Glebe, Broadening the scope of sortagging, *RSC Adv.*, 9 (9) (2019) 4700–4721, <https://doi.org/10.1039/c8ra06705h>.
- [64] J.M. Antos, M.C. Truttmann, H.L. Ploegh, Recent advances in sortase-catalyzed ligation methodology, *Curr. Opin. Struct. Biol.* 38 (2016) 111–118, <https://doi.org/10.1016/j.sbi.2016.05.021>.
- [65] L. Chen, J. Cohen, X. Song, A. Zhao, Z. Ye, C.J. Feulner, P.R. Chen, Improved variants of SrtA for site-specific conjugation on antibodies and proteins with high efficiency, *Sci. Rep.* 6 (1) (2016) 1–12, <https://doi.org/10.1038/srep31899>.
- [66] H.J. Jeong, G.C. Abhiraman, C.M. Story, J.R. Ingram, S.K. Dougan, Generation of Ca<sup>2+</sup>-independent sortase A mutants with enhanced activity for protein and cell surface labeling, *PLoS ONE* 12 (12) (2017) 1–15, <https://doi.org/10.1371/journal.pone.0189068>.
- [67] H.H. Wang, B. Altun, K. Nwe, A. Tsurukas, Proximity-Based Sortase-Mediated Ligation, *Angewandte Chemie - Int. Ed.* 56 (19) (2017) 5349–5352, <https://doi.org/10.1002/anie.201701419>.
- [68] T. Sakamoto, S. Sawamoto, T. Tanaka, H. Fukuda, A. Kondo, Enzyme-mediated site-specific antibody–protein modification using a zz domain as a linker, *Bioconjug. Chem.* 21 (12) (2010) 2227–2233, <https://doi.org/10.1021/bc100206z>.
- [69] T. Matsumoto, K. Furuta, T. Tanaka, A. Kondo, Sortase A-mediated metabolic enzyme ligation in *Escherichia coli*, *ACS Synth. Biol.* 5 (11) (2016) 1284–1289, <https://doi.org/10.1021/acssynbio.6b00194>.
- [70] S.A. McConnell, K.A. Cannon, C. Morgan, R. McAllister, B.R. Amer, R.T. Clubb, T. O. Yeates, Designed protein cages as scaffolds for building multienzyme materials, *ACS Synth. Biol.* 9 (2) (2020) 381–391, <https://doi.org/10.1021/acssynbio.9b00407>.
- [71] H. Sun, Q. Luo, C. Hou, J. Liu, Nanostructures based on protein self-assembly: from hierarchical construction to bioinspired materials, *Nano Today* 14 (2017) 16–41, <https://doi.org/10.1016/j.nantod.2017.04.006>.
- [72] Z. Liu, S. Cao, M. Liu, W. Kang, J. Xia, Self-assembled multi-enzymenanostructures on synthetic protein scaffolds, *ACS Nano* 13 (10) (2019) 11343–11352, <https://doi.org/10.1021/acsnano.9b04554>.
- [73] E. Turan, Enhanced enzyme activity with ferritin nanocages, *Hittite J. Sci. Eng.* 5 (2) (2018) 115–118, <https://doi.org/10.17350/hjse19030000081>.
- [74] Y. Zhang, B.P. Orner, Self-assembly in the ferritin nano-cage protein superfamily, *Int. J. Mol. Sci.* 12 (8) (2011) 5406–5421, <https://doi.org/10.3390/ijms12085406>.
- [75] J.L. Liu, D. Zabetakis, J.C. Breger, G.P. Anderson, E.R. Goldman, Multi-Enzyme assembly on T4 Phage Scaffold, *Front. Bioeng. Biotechnol.* 8 (2020) 571, <https://doi.org/10.3389/fbioe.2020.00571>.
- [76] C. You, Y.H.P. Zhang, Self-assembly of synthetic metabolons through synthetic protein scaffolds: one-step purification, co-immobilization, and substrate channeling, *ACS Synth. Biol.* 2 (2) (2013) 102–110, <https://doi.org/10.1021/sb300068g>.
- [77] F. Li, K. Yang, Y. Xu, Y. Qiao, Y. Yan, J. Yan, A genetically-encoded synthetic self-assembled multi-enzyme complex of lipase and P450 fatty acid decarboxylase for efficient bioproduction of fatty alkenes, *Bioresour. Technol.* 272 (2019) 451–457, <https://doi.org/10.1016/j.biortech.2018.10.067>.
- [78] T. Yu, X. Gao, Y. Ren, D. Wei, Assembly of cellulases with synthetic protein scaffolds *in vitro*, *Bioresour. Bioprocess.* 2 (1) (2015) 1–7, <https://doi.org/10.1186/s40643-015-0046-8>.
- [79] A. Heyman, Y. Barak, J. Caspi, D.B. Wilson, A. Altman, E.A. Bayer, O. Shoseyov, Multiple display of catalytic modules on a protein scaffold: nano-fabrication of enzyme particles, *J. Biotechnol.* 131 (4) (2007) 433–439, <https://doi.org/10.1016/j.jbiotec.2007.07.940>.
- [80] S. Lim, G.A. Jung, D.J. Glover, D.S. Clark, Enhanced enzyme activity through scaffolding on customizable self-assembling protein filaments, *Small* 15 (20) (2019), 1805558, <https://doi.org/10.1002/sml.201805558>.
- [81] L. Schoonen, S. Maassen, R.J. Nolte, J.C. van Hest, Stabilization of a virus-like particle and its application as a nanoreactor at physiological conditions, *Biomacromolecules* 18 (11) (2017) 3492–3497, <https://doi.org/10.1021/acs.biomac.7b00640>.
- [82] J.W. Wilkerson, S.O. Yang, P.J. Funk, S.K. Stanley, B.C. Bundy, Nanoreactors: strategies to encapsulate enzyme biocatalysts in virus-like particles, *N. Biotechnol.* 44 (2018) 59–63, <https://doi.org/10.1016/j.nbt.2018.04.003>.
- [83] M. Brasch, R.M. Putri, M.V. De Ruyter, D. Luque, M.S.T. Koay, J.R. Castón, J.J.L. M Cornelissen, Assembling enzymatic cascade pathways inside virus-based nanocages using dual-tasking nucleic acid tags, *J. Am. Chem. Soc.* 139 (4) (2017) 1512–1519, <https://doi.org/10.1021/jacs.6b10948>.
- [84] L. Lavelle, J.P. Michel, M. Gingery, The disassembly, reassembly and stability of CCMV protein capsids, *J. Virol. Methods* 146 (1–2) (2007) 311–316, <https://doi.org/10.1016/j.jviromet.2007.07.020>.
- [85] M. Comellas-Aragonès, H. Engelkamp, V.I. Claessen, N.A.J.M. Sommerdijk, A. E. Rowan, P.C.M. Christianen, R.J.M. Nolte, A virus-based single-enzyme nanoreactor, *Nat. Nanotechnol.* 2 (10) (2007) 635–639, <https://doi.org/10.1038/nnano.2007.299>.
- [86] L. Schoonen, J. Pille, A. Borrmann, R.J. Nolte, J.C. van Hest, Sortase A-mediated N-terminal modification of cowpea chlorotic mottle virus for highly efficient cargo loading, *Bioconjug. Chem.* 26 (12) (2015) 2429–2434, <https://doi.org/10.1021/acs.bioconjchem.5b00485>.
- [87] D.P. Patterson, Encapsulation of active enzymes within bacteriophage P22 virus-like particles. Protein Scaffolds, Humana Press, New York, NY, 2018, pp. 11–24, [https://doi.org/10.1007/978-1-4939-7893-9\\_2](https://doi.org/10.1007/978-1-4939-7893-9_2).
- [88] D. Patterson, B. Schwarz, J. Avera, B. Western, M. Hicks, P. Krugler, T. Douglas, Sortase-mediated ligation as a modular approach for the covalent attachment of proteins to the exterior of the bacteriophage P22 virus-like particle, *Bioconjug. Chem.* 28 (8) (2017) 2114–2124, <https://doi.org/10.1021/acs.bioconjchem.7b00296>.
- [89] D.P. Patterson, B. Schwarz, R.S. Waters, T. Gedeon, T. Douglas, Encapsulation of an enzyme cascade within the bacteriophage P22 virus-like particle, *ACS Chem. Biol.* 9 (2) (2014) 359–365, <https://doi.org/10.1021/cb4006529>.
- [90] J. Sharma, T. Douglas, Tuning the catalytic properties of P22 nanoreactors through compositional control, *Nanoscale* 12 (1) (2020) 336–346, <https://doi.org/10.1039/c9nr08348k>.
- [91] H.K. Waghvani, M. Uchida, C.Y. Fu, B. Lafrance, J. Sharma, K. McCoy, T. Douglas, Virus-like particles (VLPs) as a platform for hierarchical compartmentalization, *Biomacromolecules* 21 (6) (2020) 2060–2072, <https://doi.org/10.1021/acs.biomac.0c00030>.
- [92] G. Jutz, P. Van Rijn, B. Santos Miranda, A. Böker, Ferritin: a versatile building block for bionanotechnology, *Chem. Rev.* 115 (4) (2015) 1653–1701, <https://doi.org/10.1021/cr400011b>.
- [93] M. Kim, Y. Rho, K.S. Jin, B. Ahn, S. Jung, H. Kim, M. Ree, PH-dependent structures of ferritin and apoferritin in solution: disassembly and reassembly, *Biomacromolecules* 12 (5) (2011) 1629–1640, <https://doi.org/10.1021/bm200026v>.
- [94] Z. Wang, H. Gao, Y. Zhang, G. Liu, G. Niu, X. Chen, Functional ferritin nanoparticles for biomedical applications, *Front. Chem. Sci. Eng.* 11 (4) (2017) 633–646, <https://doi.org/10.1016/j.physbeh.2017.03.040>.
- [95] Y. Zhang, Z. Tang, J. Wang, H. Wu, C.T. Lin, Y. Lin, Apoferritin nanoparticle: a novel and biocompatible carrier for enzyme immobilization with enhanced activity and stability, *J. Mater. Chem.* 21 (43) (2011) 17468–17475, <https://doi.org/10.1039/c1jm11598g>.
- [96] A. Heyman, I. Levy, A. Altman, O. Shoseyov, SP1 as a novel scaffold building block for self-assembly nanofabrication of submicron enzymatic structures, *Nano Lett.* 7 (6) (2007) 1575–1579, <https://doi.org/10.1021/nl070450q>.
- [97] W.X. Wang, O. Dgany, S.G. Wolf, I. Levy, R. Algom, Y. Pouny, O. Shoseyov, Aspen SP1, an exceptional thermal, protease and detergent-resistant self-assembled nano-particle, *Biotechnol. Bioeng.* 95 (1) (2006) 161–168, <https://doi.org/10.1002/bit.21010>.
- [98] S. Morais, A. Heyman, Y. Barak, J. Caspi, D.B. Wilson, R. Lamed, E.A. Bayer, Enhanced cellulose degradation by nano-complexed enzymes: synergism between a scaffold-linked exoglucanase and a free endoglucanase, *J. Biotechnol.* 147 (3–4) (2010) 205–211, <https://doi.org/10.1016/j.jbiotec.2010.04.012>.
- [99] C.A. Kerfeld, C. Aussignargues, J. Zarzycki, F. Cai, M. Sutter, Bacterial microcompartments, *Nat. Rev. Microbiol.* 16 (5) (2018) 277–290, <https://doi.org/10.1038/nrmicro.2018.10>.
- [100] M. Held, A. Kolb, S. Perdue, S.Y. Hsu, S.E. Bloch, M.B. Quin, C. Schmidt-Dannert, Engineering formation of multiple recombinant, Eut protein nanocompartments in *E. coli*, *Sci. Rep.* 6 (1) (2016) 1–15, <https://doi.org/10.1038/srep24359>.
- [101] H.J. Wagner, C.C. Capitain, K. Richter, M. Nessler, J. Mampel, Engineering bacterial microcompartments with heterologous enzyme cargos, *Eng. Life Sci.* 17 (1) (2017) 36–46, <https://doi.org/10.1002/elsc.201600107>.
- [102] A.R. Hagen, J.S. Plegaria, N. Sloan, B. Ferlez, C. Aussignargues, R. Burton, C. A. Kerfeld, *In vitro* assembly of diverse bacterial microcompartment shell architectures, *Nano Lett.* 18 (11) (2018) 7030–7037, <https://doi.org/10.1021/acs.nanolett.8b02991>.
- [103] A. Hagen, M. Sutter, N. Sloan, C.A. Kerfeld, Programmed loading and rapid purification of engineered bacterial microcompartment shells, *Nat. Commun.* 9 (1) (2018) 1–10, <https://doi.org/10.1038/s41467-018-05162-z>.
- [104] M.J. Lee, J. Mantell, I.R. Brown, J.M. Fletcher, P. Verkade, R.W. Pickersgill, M. J. Warren, De novo targeting to the cytoplasmic and luminal side of bacterial microcompartments, *Nat. Commun.* 9 (1) (2018) 1–11, <https://doi.org/10.1038/s41467-018-05922-x>.

- [105] D.J. Glover, D.S. Clark, Oligomeric assembly is required for chaperone activity of the filamentous  $\gamma$ -prefoldin, *FEBS J.* 282 (15) (2015) 2985–2997, <https://doi.org/10.1111/febs.13341>.
- [106] D.J. Glover, L. Giger, J.R. Kim, D.S. Clark, Engineering protein filaments with enhanced thermostability for nanomaterials, *Biotechnol. J.* 8 (2) (2013) 228–236, <https://doi.org/10.1002/biot.201200009>.
- [107] T.K. Gła̧b, J. Boratyński, Potential of casein as a carrier for biologically active agents, *Top. Curr. Chem.* 375 (4) (2017) 1–20, <https://doi.org/10.1007/s41061-017-0158-z>.
- [108] S. Lilla, G. Mamone, Structural Characterization of transglutaminase-catalyzed casein cross-linking, *J. Chromatogr. Separation Tech.* 3 (2) (2012), 1000122, <https://doi.org/10.4172/2157-7064.1000122>.
- [109] G.A.L.G. Budinova, Y. Mori, T. Tanaka, N. Kamiya, Casein-based scaffold for artificial cellulosome design, *Process Biochem.* 66 (2018) 140–145, <https://doi.org/10.1016/j.procbio.2017.12.013>.
- [110] S.J. Jiang, X.H. Zhao, Cross-linking and glucosamine conjugation of casein by transglutaminase and the emulsifying property and digestibility *in vitro* of the modified product, *Int. J. Food Properties* 15 (6) (2012) 1286–1299, <https://doi.org/10.1080/10942912.2010.521274>.
- [111] D. Dharmadana, N.P. Reynolds, C.E. Conn, C. Valéry, Molecular interactions of amyloid nanofibrils with biological aggregation modifiers: implications for cytotoxicity mechanisms and biomaterial design, *Interface Focus* 7 (4) (2017), 20160160, <https://doi.org/10.1098/rsfs.2016.0160>.
- [112] C.L.L. Pham, A.H. Kwan, M. Sunde, Functional amyloid: widespread in nature, diverse in purpose, *Essays Biochem.* 56 (1) (2014) 207–219, <https://doi.org/10.1042/BSE0560207>.
- [113] S. Chaves, L.M. Pera, C.L. Avila, C.M. Romero, M. Baigori, F.E.M. Vieyra, R. N. Chehin, Towards efficient biocatalysts: photo-immobilization of a lipase on novel lysozyme amyloid-like nanofibrils, *RSC Adv.* 6 (11) (2016) 8528–8538, <https://doi.org/10.1039/c5ra19590j>.
- [114] B. Schmuck, M. Gudmundsson, T. Hård, M. Sandgren, Coupled chemistry kinetics demonstrate the utility of functionalized Sup35 amyloid nanofibrils in biocatalytic cascades, *J. Biol. Chem.* 294 (41) (2019) 14966–14977, <https://doi.org/10.1074/jbc.RA119.008455>.
- [115] H.-I. Jung, S.J. Bowden, A. Cooper, R.N. Perham, Thermodynamic analysis of the binding of component enzymes in the assembly of the pyruvate dehydrogenase multi-enzyme complex of *Bacillus stearothermophilus*, *Protein Sci.* 11 (5) (2002) 1091–1100, <https://doi.org/10.1110/ps.4970102>.
- [116] I.B. Durowoju, K.S. Bhandal, J. Hu, B. Carpick, M. Kirkitadze, Differential scanning calorimetry — A method for assessing the thermal stability and conformation of protein antigen, *J. Visualized Experiments* (121) (2017) e55262, <https://doi.org/10.3791/55262>.
- [117] M.H. Chiu, E.J. Prenner, Differential scanning calorimetry: an invaluable tool for a detailed thermodynamic characterization of macromolecules and their interactions, *J. Pharm. Bioallied Sci.* 3 (1) (2011) 39–59, <https://doi.org/10.4103/0975-7406.76463>.
- [118] J. Boeckx, M. Hertog, A. Geeraerd, B. Nicolai, Kinetic modelling: an integrated approach to analyze enzyme activity assays, *Plant Methods* 13 (1) (2017) 1–12, <https://doi.org/10.1186/s13007-017-0218-y>.
- [119] Y. Wang, G. Wang, N. Moitessier, A.K. Mittermaier, Enzyme kinetics by isothermal titration calorimetry: allostery, inhibition, and dynamics, *Front Mol. Biosci.* 7 (2020), 583826, <https://doi.org/10.3389/fmolb.2020.583826>.
- [120] Q. Yu, Y. Wang, S. Zhao, Y. Ren, Photocontrolled reversible self-assembly of dodecamer nitrilase, *Bioresour. Bioprocess.* 4 (1) (2017) 2–9, <https://doi.org/10.1186/s40643-017-0167-3>.
- [121] G. Zhang, S. Schmidt-Dannert, M.B. Quin, C. Schmidt-Dannert, Protein-based scaffolds for enzyme immobilization, *Meth. Enzymol.* 617 (2019) 323–362, <https://doi.org/10.1016/bs.mie.2018.12.016>.
- [122] Arzenšek, D., Podgornik, R., & Kuzman, D. (2010). Dynamic light scattering and application to proteins in solutions. In Seminar; University of Ljubljana: Ljubljana, Slovenia (pp. 1–18). 10.3867/j.issn.1000-3002.2013.03.007.
- [123] M.A. Al-Ghobashy, M.M. Mostafa, H.S. Abed, F.A. Fathalla, M.Y. Salem, Correlation between dynamic light scattering and size exclusion high performance liquid chromatography for monitoring the effect of pH on stability of biopharmaceuticals, *J. Chromatography B* 1060 (2017) 1–9, <https://doi.org/10.1016/j.jchromb.2017.05.029>.
- [124] S. Averick, O. Karácsy, J. Mohin, X. Yong, N.M. Moellers, B.F. Woodman, K. Matyjaszewski, Cooperative, reversible self-assembly of covalently pre-linked proteins into giant fibrous structures, *Angewandte Chemie - Int. Ed.* 53 (31) (2014) 8050–8055, <https://doi.org/10.1002/anie.201402827>.
- [125] L. Orellana, Large-Scale Conformational Changes and protein function: breaking the *in silico* barrier, *Front. Mol. Biosci.* 6 (2019) 117, <https://doi.org/10.3389/fmolb.2019.00117>.
- [126] N. Plattner, S. Doerr, G. De Fabritiis, F. Noé, Complete protein-protein association kinetics in atomic detail revealed by molecular dynamics simulations and Markov modelling, *Nat. Chem.* 9 (10) (2017) 1005–1011, <https://doi.org/10.1038/nchem.2785>.
- [127] Y. Kodama, C.D. Hu, Bimolecular fluorescence complementation (BiFC): a 5-year update and future perspectives, *BioTechniques* 53 (5) (2012) 285–298, <https://doi.org/10.2144/000113943>.
- [128] Y. Hua, J. Ju, X. Wang, B. Zhang, W. Zhao, Q. Zhang, C. Wan, Screening for host proteins interacting with *Escherichia coli* O157:H7 EspF using bimolecular fluorescence complementation, *Future Microbiol.* 13 (1) (2018) 37–58, <https://doi.org/10.2217/fmb-2017-0087>.
- [129] S. Dey, A. Anbanandam, B.E. Mumford, R.N. De Guzman, Characterization of small-molecule scaffolds that bind to the shigella type iii secretion system protein IpaD, *Chem. Med. Chem.* 12 (18) (2017) 1534–1541, <https://doi.org/10.1002/cmdc.201700348>.
- [130] S.P. Smith, E.A. Bayer, M. Czjzek, Continually emerging mechanistic complexity of the multi-enzyme cellulosome complex, *Curr. Opin. Struct. Biol.* 44 (2017) 151–160, <https://doi.org/10.1016/j.sbi.2017.03.009>.
- [131] D. Luque, J.R. Castón, Cryo-electron microscopy for the study of virus assembly, *Nat. Chem. Biol.* 16 (3) (2020) 231–239, <https://doi.org/10.1038/s41589-020-0477-1>.
- [132] L. Ciccarelli, S.R. Connell, M. Enderle, D.J. Mills, J. Vonck, M. Gringer, Structure and conformational variability of the mycobacterium tuberculosis fatty acid synthase multi-enzyme complex, *Structure* 21 (7) (2013) 1251–1257, <https://doi.org/10.1016/j.str.2013.04.023>.
- [133] G. Skinnotis, D.R. Southworth, Single-particle cryo-electron microscopy of macromolecular complexes, *Microscopy* 65 (1) (2016) 9–22, <https://doi.org/10.1093/jmicro/dfv366>.
- [134] M. Qian, S. Guan, Y. Shan, H. Zhang, S. Wang, Structural and molecular basis of cellulase Cel48F by computational modeling: insight into catalytic and product release mechanism, *J. Struct. Biol.* 194 (3) (2016) 347–356, <https://doi.org/10.1016/j.jsb.2016.03.012>.